NATIONAL ADVISORY COMMITTEE FOR AERONAUTICS

TECHNICAL NOTE 3335

METHODS FOR RAPID GRAPHICAL EVALUATION OF COOLED OR UNCOOLED TURBOJET AND TURBOPROP ENGINE OR COMPONENT PERFORMANCE (EFFECTS OF VARIABLE SPECIFIC HEAT INCLUDED)

By Jack B. Esgar and Robert R. Ziemer

Lewis Flight Propulsion Laboratory
Cleveland, Ohio

Washington
January 1955

M

NATIONAL ADVISORY COMMITTEE FOR AERONAUTICS

TECHNICAL NOTE 3335

METHODS FOR RAPID GRAPHICAL EVALUATION OF COOLED OR UNCOOLED TURBOJET AND TURBOPROP ENGINE OR COMPONENT PERFORMANCE (EFFECTS OF VARIABLE SPECIFIC HEAT INCLUDED)

By Jack B. Esgar and Robert R. Ziemer

SUMMARY

In order to simplify and accelerate calculation procedures for component or over-all cycle performance of gas-turbine engines, a series of curves was prepared relating the parameters affecting each engine component. These curves are based on the thermodynamic properties of air and combustion gases for a hydrogen-carbon ratio of 0.167, which is generally applicable for jet-engine fuels. The effects of variations in specific heat during each process in the components are also included. The curves cover a range of flight Mach numbers from zero to 3.0, compressor pressure ratios from 1 to 30, turbine-inlet temperatures from 1500° to 3000° R, and afterburner temperatures from 2800° to 3500° R. Except for extreme cases, the curves are accurate at a hydrogen-carbon ratio of 0.167 to at least 3° R in temperature and 1 percent in pressure ratio, fuel-air ratio, and specific thrust. For hydrogen-carbon ratios considerably different from 0.167 (in the range from 0.1 to 0.2), somewhat larger errors are possible. The curves are adequate, however, for nearly all cycle or component analyses and reduction of experimental data for gas temperatures up to 3000° R. For gas temperatures in excess of 3000° R, the curves should be used with caution, because the effects of dissociation were neglected. Procedures required for performance evaluation are explained for both uncooled engines with no compressor bleed and for engines utilizing both compressor bleed and turbine cooling.

INTRODUCTION

Procedures available for accurate cycle calculations to determine engine performance depend on the use of tables or charts of the thermodynamic properties of air and combustion gases. Calculations made in this manner are usually cumbersome and time-consuming. In order to simplify and accelerate calculation procedures, a series of curves was prepared and a calculation procedure devised to provide a quick and accurate

method of determining component or engine performance for gas-turbine power plants. Desirable features of graphical solutions, in addition to simplicity, are that the method used be sufficiently accurate and that the methods be adaptable to a wide variety of components and operating conditions.

Graphical solutions employed by previous investigators (refs. 1 to 3) served the purpose intended, but different solutions are desirable when accounting for turbine cooling in component or engine performance. In addition, the effects of variable specific heat were not included in reference 1. While in some cases the effects of variations in specific heat are small, greater accuracy is obtainable if the effects of variations are included, particularly for processes where the change in temperature in the process is large. In references 2 and 3, corrections were used to account for specific-heat variations, but the performance of several components was often grouped together so that it is difficult to evaluate the performance of a single component or to calculate engine performance where part of the compressor air is bled for turbine cooling or other purposes. The charts in reference 4, which include effects of variations in specific heat, provide an accurate method for cycle or component analysis; but the use of simple curves for graphically obtaining the performance of each component can greatly simplify the calculation procedure. For this reason the data presented in reference 4 were used for the preparation of curves in this report. These curves provide a quick and accurate method of obtaining component performance. By combining the component performances obtained graphically, the over-all cycle performance is easily obtained. Calculation procedures were devised for a wide variety of operating conditions that include most modes of engine operation including bleeding of the compressor for turbine cooling or other purposes.

The range of variables covered by the curves are flight Mach numbers from zero to 3.0, compressor pressure ratios from 1 to 30, turbine-inlet temperatures from 1500° to 3000° R, and afterburner temperatures from 2800° to 3500° R. In addition, charts are provided so that either adiabatic or polytropic efficiencies can be considered in the compressor and turbine.

PREPARATION OF CHARTS

This section presents the calculation methods required for preparing the curves used for graphical evaluation of engine components. (The equations used in this section of the report are not needed in order to use the curves; they are only needed to obtain the curves.) In all cases where either one or several equations specify the relation between the variables involved in a specific process, numerical values were assigned to all but one of the variables. The unknown quantity was then computed

using the appropriate equations, and the curves were constructed. The symbols used throughout the report are defined in appendix A, and the numerical subscripts refer to the stations in the engine shown in figure 1.

Ram Temperature and Pressure

The enthalpy rise due to ram can be expressed by

$$h_0' - h_0 = \frac{V_0^2}{2gJ} \tag{1}$$

By expressing velocity as a function of flight Mach number, equation (1) becomes

$$h_0' - h_0 = \frac{M_0^2 \gamma_0 R T_0}{2J} \tag{2}$$

By using charts in reference 4 to convert from enthalpies to temperatures and obtaining the ratio of specific heats from reference 5, the ram temperature ratio can be calculated. There is no change in total temperature between stations 0 and 1 (see fig. 1 for station locations); therefore, since $T_1' = T_0'$, equation (2) can be used for calculating θ_1, which is defined as

$$\theta_1 = \frac{T_1'}{518.7} \tag{3}$$

Figure 2 shows θ_1 plotted against flight Mach number for a range of altitudes at NACA standard temperature.

The isentropic pressure rise due to ram can be obtained from the following equation, which is derived in appendix B:

$$\frac{p_0'}{p_0} = e^{\frac{J}{R}(\varphi_0' - \varphi_0)} \tag{4}$$

where the values of φ_0' and φ_0 correspond to values of h_0' and h_0, respectively, from equation (2) and can be read from charts in reference 4. The isentropic ram pressure ratio is plotted against flight Mach number in figure 3 for a range of standard temperatures at altitude.

Compressor Work

Based on adiabatic compressor efficiency. - The compressor equivalent specific work is defined as

$$\frac{\Delta h_C'}{\theta_1} \equiv \frac{h_2' - h_1'}{\theta_1} \tag{5}$$

and the adiabatic efficiency of a compression process is defined by

$$\eta_C \equiv \frac{h_{2,i}' - h_1'}{h_2' - h_1'} \tag{6}$$

Combining equations (5) and (6) results in an equivalent specific work parameter defined as

$$\frac{\eta_C \Delta h_C'}{\theta_1} \equiv \frac{h_{2,i}' - h_1'}{\theta_1} \tag{7}$$

Given values of inlet temperature T_1' will result in corresponding values of h_1' and φ_1', which can be read from the charts of reference 4. For various values of compressor pressure ratio p_2'/p_1' and the following equation derived in appendix B,

$$\varphi_{2,i}' - \varphi_1' = \frac{R}{J} \ln\left(\frac{p_2'}{p_1'}\right) \tag{8}$$

values of $\varphi_{2,i}'$ can be calculated. Using values of the isentropic enthalpy $h_{2,i}'$ at the compressor discharge corresponding to values of $\varphi_{2,i}'$ permits calculation of the compressor equivalent specific work parameter from equation (7) for ranges of p_2'/p_1' and θ_1. The results of these calculations are presented in figure 4.

Based on polytropic compressor efficiency. - To obtain the compressor equivalent specific work as defined in equation (5), values of enthalpy are obtained corresponding to the inlet temperature T_1' and the value of φ_2'. The value φ_2', which is a function of compressor pressure ratio p_2'/p_1' and polytropic efficiency $\eta_{C,\infty}$, is calculated from the following equation (see appendix B):

$$\varphi_2' - \varphi_1' = \frac{R}{J} \ln\left(\frac{p_2'}{p_1'}\right)^{\frac{1}{\eta_{C,\infty}}} \tag{9}$$

Comparison of equations (5) to (9) shows that a single curve can be used for representing the compressor equivalent specific work as a function of compressor pressure ratio and inlet temperature for both adiabatic and polytropic efficiencies by use of the proper ordinates and abscissas. Thus, the results of the calculations for compressor work based on polytropic compressor efficiency are also presented in figure 4. An additional set of curves is provided at the top of the figure for quick conversion from p_2'/p_1' to $(p_2'/p_1')^{\frac{1}{\eta_{C,\infty}}}$ for representative values of polytropic efficiency $\eta_{C,\infty}$. In order to eliminate the necessity for interpolation for values of $\eta_{C,\infty}$ not given on the curve, the upper abscissa can, of course, be easily calculated from given values of $\eta_{C,\infty}$ and p_2'/p_1'.

Compressor Temperature Ratio

Equation (5) can be written

$$\frac{h_2'}{h_1'} \equiv 1 + \frac{\theta_1}{h_1'} \frac{\Delta h_C'}{\theta_1} \tag{10}$$

By conversion from enthalpies h' to temperatures T', the compressor temperature ratio can be expressed as a function of the compressor equivalent specific work and the compressor-inlet equivalent temperature. Such a relation is expressed graphically in figure 5.

Fuel-Air Ratio

The total fuel-air ratio at the burner exit for a combustion process that includes the effect of fuel burned in a previous combustion process is derived in appendix B:

$$\left(\frac{f}{a}\right)_\beta = \left(\frac{f}{a}\right)_\alpha + \frac{X\left[1 + \left(\frac{f}{a}\right)_\alpha Y\right]}{\eta_B Z} \tag{B18}$$

where

$$X = h'_{A,\beta} - h'_{A,\alpha}$$

$$Y = \frac{h'_{A,\beta} - h'_{A,\alpha} + \psi'_{h,\beta} - \psi'_{h,\alpha}}{h'_{A,\beta} - h'_{A,\alpha}}$$

$$Z = \overline{H} - \frac{h'_{A,\beta} + \psi'_{h,\beta} - h_f}{\eta_B}$$

For the case where there was no fuel burned previously, $(f/a)_\alpha = 0$, and equation (B18) can be written

$$\eta_B\left(\frac{f}{a}\right)_\beta = \frac{X}{Z} \tag{11}$$

To obtain an equation similar to equation (11) for the case of two or more combustion processes in series, equation (B18) can be rewritten as

$$\eta_B\left(\frac{f}{a}\right)^* = \frac{X}{Z} \tag{12}$$

where

$$\left(\frac{f}{a}\right)^* \equiv \frac{\left(\frac{f}{a}\right)_\beta - \left(\frac{f}{a}\right)_\alpha}{1 + \left(\frac{f}{a}\right)_\alpha Y} \tag{13}$$

The use of the term Y is involved only for two or more combustion processes in series, as would be the case with an afterburner. It has been found that, for afterburner-outlet temperatures up to 3500° R, afterburner-inlet temperatures from 1500° to 3000° R, and a hydrogen-carbon ratio of 0.167, $Y \approx 2.9$ with a maximum variation of ±5 percent. In equations (11) and (12), the value of Y is multiplied by the fuel-air ratio at the inlet to the second burner (which will generally be $0 < (f/a)_\alpha < 0.05$) and then added to 1. By assigning a constant value of $Y = 2.9$, the maximum error in total fuel-air ratio up to stoichiometric will be less than 0.2 percent.

Equations (11) and (12) and the charts in reference 4 were used to obtain figure 6, with the appropriate subscripts for stations shown in figure 1. Figure 6 is a plot of the product of the combustion efficiency and fuel-air ratio $\eta_{B,2\text{-}3}(f/a)_3$ or $\eta_{B,5\text{-}6}(f/a)^*$ plotted against

burner-inlet equivalent temperature θ_2 or θ_5 with burner-outlet temperature T_3' or T_6' as a parameter for two values of burner efficiency (a small effect in the type of plot used). For the subscripts used in figure 6, the fuel air-ratio designated $(f/a)^*$ is defined

$$\left(\frac{f}{a}\right)^* \equiv \frac{\left(\frac{f}{a}\right)_6 - \left(\frac{f}{a}\right)_5}{1 + 2.9\left(\frac{f}{a}\right)_5} \tag{14}$$

It should be noted that the burner efficiency η_B does not have to be the same for the first and second burners. In addition, the fuel-air ratio at station 5 may not be the same as the fuel-air ratio at station 3 because of the addition of bleed air to dilute the gases.

Figure 6 was obtained from calculations in which it was assumed that the fuel temperature was 540° R and the hydrogen-carbon ratio H/C was 0.167, resulting in a fuel lower heating value $\overline{H}$ of 18,562 Btu per pound of fuel. Fuel temperature has a negligible effect on fuel-air ratio. Each 100° R increase in fuel temperature will decrease the fuel-air ratio about 0.3 percent. For values of H/C different from 0.167, the fuel-air ratio can be closely approximated by dividing the fuel-air ratio obtained from figure 6 by the quantity 0.670 H/C + 0.888. This correction factor was obtained by determining analytically that the value of Z in equations (11) and (13) can be very closely approximated by the expression

$$Z = Z_{H/C} = 0.167\left(0.670\,\frac{H}{C} + 0.888\right) \tag{15}$$

for hydrogen-carbon ratios from 0.1 to 0.2 and for burner-outlet temperatures from 2000° to 3500° R. The maximum error (0.4 percent) occurs at a hydrogen-carbon ratio of 0.1 at a burner-outlet temperature of 3500° R.

Turbine Temperature Ratio

The turbine temperature ratio θ_4/θ_3 is a function of the turbine work and the specific heat of the gas. The turbine equivalent specific work is defined as

$$\frac{\Delta h_T'}{\theta_3} \equiv \frac{h_3' - h_4'}{\theta_3} \tag{16}$$

This equation can be rearranged to the form

$$\frac{h_4'}{h_3'} \equiv 1 - \left(\frac{\theta_3}{h_3'}\frac{\Delta h_T'}{\theta_3}\right) \tag{17}$$

By use of equation (17) and the charts in reference 4 for converting from enthalpies to temperatures, the turbine temperature ratio θ_4/θ_3 can be calculated for a range of turbine work values. In addition, both temperature level, designated by θ_3, and fuel-air ratio will affect the turbine temperature ratio because of their effect on the specific heat of the gas. The results of calculations for turbine temperature ratio are plotted in figure 7 against turbine equivalent specific work $\Delta h_T'/\theta_3$ for a range of fuel-air ratios $(f/a)_3$ from 0.01 to 0.04 and equivalent turbine-inlet temperatures θ_3 from 3 to 6. If necessary, the curves can be used for values of fuel-air ratio less than 0.01 by extrapolation.

Turbine Work

Based on adiabatic turbine efficiency. - The adiabatic efficiency of an expansion process is defined by

$$\eta_T \equiv \frac{h_3' - h_4'}{h_3' - h_{4,i}'} \tag{18}$$

The combination of equations (16) and (18) results in an equivalent specific work parameter of the same general type as the one used for the compressor:

$$\frac{\Delta h_T'}{\eta_T \theta_3} = \frac{h_3' - h_{4,i}'}{\theta_3} \tag{19}$$

Using the following equation derived in appendix B,

$$\varphi_{4,i}' - \varphi_3' = \frac{R}{J} \ln\left(\frac{p_4'}{p_3'}\right) \tag{20}$$

and a procedure similar to that used for obtaining the compressor work curve based on adiabatic efficiency, curves in figure 8 were calculated and plotted. For the turbine there is one additional variable, fuel-air ratio, that must also be accounted for because of its effect on specific heat of the gas. The effect of fuel-air ratio is handled in the same way in figure 8 as it was in figure 7.

Based on polytropic turbine efficiency. - The relation between turbine pressure ratio and turbine work for the case where polytropic turbine efficiency is used is handled in a manner similar to that for the compressor, except that equation (16) and the following equation are utilized:

$$\varphi_4' - \varphi_3' = \frac{R}{J} \ln\left(\frac{p_4'}{p_3'}\right)^{\eta_{T,\infty}} \tag{21}$$

Equation (21) is derived in appendix B.

From these calculations, a plot (fig. 8) can be used for expressing turbine equivalent specific work as a function of turbine pressure ratio for a range of turbine-inlet temperature and fuel-air ratio for both adiabatic and polytropic turbine efficiency in a manner similar to that used for the compressor.

Specific Thrust

Convergent-divergent nozzle. - The gross thrust from a jet nozzle is expressed by

$$F = \frac{w_7}{g} V_7 \tag{22}$$

where V_7 is the axial component of the jet velocity. For most cases the nozzle divergence angle is low enough that radial components of velocity can be neglected. As shown in reference 6, a divergence angle of 15° would result in an axial-velocity loss of only $1\frac{1}{2}$ percent. The jet velocity can be obtained from the expression

$$V_7 = \sqrt{2gJ(h_6' - h_7)} \tag{23}$$

The exhaust-nozzle efficiency is defined as

$$\eta_n \equiv \frac{h_6' - h_7}{h_6' - h_{7,i}} \tag{24}$$

Combining equations (23) and (24) results in

$$V_7 = \sqrt{2gJ(h_6' - h_{7,i})\eta_n} \tag{25}$$

where $h_{7,i}$ is the static enthalpy that would be obtained with an isentropic expansion. This value corresponds to the value of $\varphi_{7,i}$ obtained from the following equation derived in appendix B:

$$\varphi_6' - \varphi_{7,i} = \frac{R}{J} \ln\left(\frac{p_6'}{p_7}\right) \tag{26}$$

By combining equations (22) and (25) and remembering that $w_6 = w_7$, a gross specific thrust parameter can be obtained:

$$\frac{F}{w_6 \sqrt{\theta_6 \eta_n}} = \sqrt{\frac{2J}{g}\left(\frac{h_6' - h_{7,i}}{\theta_6}\right)} \tag{27}$$

Values of this parameter were calculated for a range of pressure ratios across the jet nozzle, where it was assumed that $p_7 = p_0$. Both fuel-air ratio and temperature level affect the specific heat of the gas and therefore have an effect on the gross thrust parameter. In figure 9 curves of the gross specific thrust parameter $F^*/w_6\sqrt{\theta_6\eta_n}$ at a fuel-air ratio of 0.01 are plotted against the exhaust-nozzle pressure ratio p_6'/p_0 with equivalent exhaust-nozzle temperature θ_6 as a parameter. The effect of fuel-air ratio different from 0.01 may be accounted for by a correction factor C, which is defined as

$$C = \frac{\dfrac{F}{w_6\sqrt{\theta_6\eta_n}}}{\dfrac{F^*}{w_6\sqrt{\theta_6\eta_n}}} \tag{28}$$

Convergent nozzle. - For a convergent nozzle, the maximum velocity is sonic and the minimum pressure at the nozzle exit is the critical pressure. For expansion ratios across the nozzle p_6'/p_0 in excess of the critical pressure ratio (about 2) the gross thrust results from both jet velocity and pressure forces and is expressed by the equation

$$F = \frac{w_7 V_7}{g} + A_7 (p_7 - p_0) \tag{29}$$

For expansion ratios less than the critical, there are no pressure forces; therefore, the thrust is calculated in exactly the same manner as for a convergent-divergent nozzle. The discussion here will consider

only the case for supercritical pressure ratios. For a supercritical pressure ratio across a convergent nozzle, the jet velocity at the nozzle exit is sonic and can be calculated from

$$V_7 = \sqrt{\gamma_7 g R T_7} \tag{30}$$

where the static temperature T_7 at sonic velocity can be obtained by iteration from the expression

$$h_6' - h_7 = \frac{\gamma_7 R T_7}{2J} \tag{31}$$

Approximately the same accuracy can be obtained, however, from a simpler iteration of the expression

$$T_7 = T_6'\left(\frac{2}{\gamma+1}\right) \tag{32}$$

where the ratio of specific heats γ is read from reference 5, and the evaluation is made by iteration for the mean temperature $(T_6' + T_7)/2$.

The thrust obtained from pressure forces is a function of the nozzle-exit static pressure p_7, which is a function of the nozzle efficiency as defined in equation (24). The procedure for calculating p_7 is as follows: The isentropic enthalpy at the nozzle exit is determined from the total temperature at station 6, the static temperature at station 7 as determined from equation (31) or (32), and equation (24) for nozzle efficiency. Converting temperatures or enthalpies to values of φ and use of the following equation (derived in appendix B)

$$\frac{p_6'}{p_7} = e^{\frac{J}{R}(\varphi_6' - \varphi_{7,i})} \tag{33}$$

provides a method of evaluating the exhaust-nozzle-exit static pressure p_7.

The flow area of the exhaust nozzle can be written

$$A_7 = \frac{w_7}{\rho_7 V_7} = \frac{w_7 R T_7}{p_7 V_7} \tag{34}$$

Combining equations (29), (30), and (34) and remembering that $w_6 = w_7$ yield an expression for gross specific thrust:

$$\frac{F}{w_6\sqrt{\theta_6}} = \frac{1}{\sqrt{\theta_6}}\left[\frac{V_7}{g} + \frac{RT_7}{V_7}\left(1 - \frac{p_0}{p_7}\right)\right] \tag{35}$$

where

$$\frac{p_0}{p_7} \equiv \frac{p_6'/p_7}{p_6'/p_0} \tag{36}$$

Values of the gross specific thrust for a convergent nozzle were calculated for ranges of exhaust-nozzle pressure ratio p_6'/p_0, equivalent temperature θ_6, and fuel-air ratio $(f/a)_6$. In figure 10 curves of gross specific thrust $F^*/w_6\sqrt{\theta_6}$ at a fuel-air ratio of 0.01 and θ_6 of 3.0 are plotted against exhaust-nozzle pressure ratio p_6'/p_0 with exhaust-nozzle efficiency η_n as a parameter. The effects of fuel-air ratio and equivalent temperature may be accounted for by a correction factor $\overline{C}$ which is defined as

$$\overline{C} = \frac{\dfrac{F}{w_6\sqrt{\theta_6}}}{\dfrac{F^*}{w_6\sqrt{\theta_6}}} \tag{37}$$

This correction factor is independent of expansion ratio.

At pressure ratios up to somewhat higher than the critical pressure ratio, the thrust is the same for both convergent and convergent-divergent exhaust nozzles. For this reason, figure 9 is applicable for both types of nozzles up to expansion ratios of 2.0. Since a different type of correction factor is required for the convergent nozzle at expansion ratios less than 2.0, the curves in figure 10 are terminated at that point.

ACCURACY OF CURVES

All the curves (figs. 2 to 10) were obtained from calculations that made use of the charts in reference 4. The charts in reference 4 are easily read to within 1° R for dry air and to within 2.5° R for combustion gases with a hydrogen-carbon ratio of 0.167. For a fuel hydrogen-carbon ratio of 0.167, the accuracy of the curves presented herein is somewhat lower than that in reference 4 and is generally limited by the scales on the figures, except for figure 7 (dealing with the turbine) where somewhat larger errors are occasionally involved because of

necessary fairing to obtain readily usable curves. In all cases the accuracy is generally better than that obtainable for experimental data, is generally as good as or better than slide-rule accuracy, and is completely adequate for nearly all cycle or component analyses. For fuel hydrogen-carbon ratios different from 0.167, larger errors sometimes occur, which will be discussed later. The effects of dissociation at high temperatures were neglected both in reference 4 and in this report; consequently, the curves should be used with caution at gas temperatures in excess of 3000° R.

The following table lists the maximum errors in each of the curves for a hydrogen-carbon ratio of 0.167; in general, the accuracy is better than that indicated:

Figure	Engine component	Maximum error
2	Inlet	3° R
3	Inlet	1 Percent
4	Compressor[a]	$2\frac{1}{2}^{\circ}$ R
5	Compressor	3° R
6	Burner[a]	0.1 To 0.5 percent
7	Turbine[a]	3° R In reading 10° R In curve fairing
8	Turbine[a]	1 Percent
9	Nozzle[a]	0.5 Percent
10	Nozzle[a]	0.3 Percent

[a]See comments in discussion following.

The possible error of $2\frac{1}{2}^{\circ}$ R in figure 4 refers to the reading error in the turbine equivalent work parameter. The scale on the figure permits reading to a value of $\Delta h'$ to within 0.5 Btu per pound, which corresponds to approximately $2\frac{1}{2}^{\circ}$ R.

As stated in the section on PREPARATION OF CHARTS, approximations were made in the calculation of fuel-air ratio. In general, all the approximations are of smaller magnitude than the reading accuracy in figure 6, which, of course, varies along the scale with the best percentage accuracy at high fuel-air ratios. For single combustors the maximum error in fuel-air ratio after applying a correction for hydrogen-carbon ratio is 0.4 percent at a hydrogen-carbon ratio of 0.1. Such a low value of hydrogen-carbon ratio is of little interest, because most hydrogen-carbon fuels lie within the range of 0.14 to 0.19, with the average for turbojet-engine fuels very close to 0.167. For two or more combustors in series - such as for an engine with an afterburner - the value of the quantity Y

varies as much as 17 percent from the value of 2.9 used in equation (14). This variation in Y, which occurs at a hydrogen-carbon ratio of 0.1, results in a maximum error in calculation of total fuel-air ratio of only 0.7 percent. In addition, this error is in a compensating direction to other errors caused by hydrogen-carbon ratio, so that the total error due to hydrogen-carbon ratio (as affecting both Z and Y) is on the order of 0.3 percent.

In figure 7, for a hydrogen-carbon ratio of 0.167, the curves are accurate to within the reading accuracy for all equivalent inlet temperatures at a fuel-air ratio of 0.01, and at all fuel-air ratios at an equivalent inlet temperature of 4. Slight errors can exist at other combinations of inlet temperature and fuel-air ratio. The maximum error at a hydrogen-carbon ratio of 0.167 is 10° R, which occurs for a fuel-air ratio of 0.04 at an equivalent inlet temperature of 6 and an equivalent turbine work of 72 Btu per pound.

For hydrogen-carbon ratios different from 0.167, additional errors can occur. For the hydrogen-carbon ratio range from 0.1 to 0.2, the maximum combined errors, which occur at high turbine work, high temperatures, and high fuel-air ratios, can result in errors up to 22° R. For current jet-engine fuels ($0.14 < H/C < 0.19$), this maximum error is 18° R, occurring at high hydrogen-carbon ratios.

The turbine pressure ratio, plotted in figure 8, is also affected by hydrogen-carbon ratio. Again, the largest errors occur at high values of turbine work, turbine-inlet temperatures, and fuel-air ratios. The maximum errors in the pressure ratio p_4'/p_3' are listed in the following table for a range of hydrogen-carbon ratios:

H/C	Maximum error in p_4'/p_3', percent
0.10	-5.6
.14	-2.8
.19	1.2
.20	2.1

The reason for the difference in the values of the accuracy for the two nozzle curves (figs. 9 and 10) in the first table is that the curves are extended to lower values of equivalent thrust for the convergent-divergent nozzle (fig. 9). At these lower numerical values, the scale readings can result in reading errors of a larger percentage. In many cases the correction factors C and $\overline{C}$ in figures 9 and 10 can be neglected, because the magnitude of the correction is often less than the reading accuracy of the curves. Slight errors also result from use of

hydrogen-carbon ratios different from 0.167. These errors are largest at high temperatures, high fuel-air ratios, and large expansion ratios. For a range of hydrogen-carbon ratios from 0.1 to 0.2, the maximum error is a little less than 1 percent in figure 9 and about 0.4 percent in figure 10.

USE OF CURVES AND CALCULATION PROCEDURE

The curves can be used for calculation of component performance as well as over-all engine performance. The discussion of the use of the charts deals with engine performance for both turbojet and turboprop engines; from this the use of the charts for component performance is obvious.

For many applications consideration is not given to bleeding air from the compressor for cooling or other purposes. For this case the calculation procedure is greatly simplified. In this discussion, therefore, the procedure for the case with no bleed and no turbine cooling is described first, and in the following section the procedure that accounts for compressor bleed and turbine cooling is described.

Cycle Calculations without Compressor Bleed or Turbine Cooling

Compressor-inlet conditions. - The compressor-inlet temperature, given by the equivalent temperature θ_1, can be read as a function of flight Mach number and flight altitude from figure 2. The isentropic pressure ratio for the inlet diffuser p_0'/p_0 can be read as a function of flight Mach number from figure 3. There is a very slight effect of inlet temperature (as influenced by altitude) on this pressure ratio at high Mach numbers. The pressure ratio at the inlet to the compressor is obtained from the equation

$$\frac{p_1'}{p_0} \equiv \frac{p_0'}{p_0}\frac{p_1'}{p_0'} \tag{38}$$

where p_1'/p_0' is the ram recovery and is a function of the inlet diffuser configuration and the flight Mach number.

Compressor work and temperature ratio. - The method of determining compressor work differs depending on whether an adiabatic or polytropic compressor efficiency is used. In both cases, however, the work is read from figure 4. For the case where an adiabatic efficiency is used, the compressor work parameter $\eta_C \Delta h_C'/\theta_1$ is read as a function of the

pressure ratio p_2'/p_1' and θ_1 from the figure. In this case the equivalent specific compressor work is calculated from

$$\frac{\Delta h_C'}{\theta_1} \equiv \frac{1}{\eta_C} \frac{\eta_C \Delta h_C'}{\theta_1} \tag{39}$$

For the case where a polytropic compressor efficiency is used, two procedures are possible. Starting with the compressor pressure ratio p_2'/p_1', the value of $(p_2'/p_1')^{\frac{1}{\eta_{C,\infty}}}$ can be obtained from the top curve corresponding to the polytropic efficiency $\eta_{C,\infty}$ and from this the equivalent specific compressor work $\Delta h_C'/\theta_1$ can be read directly for the proper value of inlet equivalent temperature θ_1. In order to eliminate the possibility of having to interpolate for values of efficiency $\eta_{C,\infty}$ not given on the curve, the term $(p_2'/p_1')^{\frac{1}{\eta_{C,\infty}}}$ can be calculated, and then the value of $\Delta h_C'/\theta_1$ can be read from the curve.

After determination of the equivalent specific work $\Delta h_C'/\theta_1$ using either adiabatic or polytropic efficiency, the compressor temperature ratio θ_2/θ_1 can be read from figure 5 as a function of equivalent specific work $\Delta h_C'/\theta_1$ and the equivalent inlet temperature θ_1.

Primary-burner fuel-air ratio. - The fuel-air ratio is obtained through use of figure 6 for a specified turbine-inlet temperature T_3', where

$$\theta_2 \equiv \theta_1 \frac{\theta_2}{\theta_1} \tag{40}$$

and

$$\left(\frac{f}{a}\right)_3 \equiv \frac{\eta_{B,2\text{-}3}\left(\frac{f}{a}\right)_3}{\eta_{B,2\text{-}3}} \tag{41}$$

As stated previously, figure 6 was obtained for a hydrocarbon-carbon ratio H/C of 0.167. It is possible to closely approximate the fuel-air ratios that would be obtained for hydrogen-carbon ratios different from 0.167 by dividing the value of fuel-air ratio obtained from the curve by the quantity 0.670 H/C + 0.888.

Turbojet-engine turbine work and temperature ratio. - The total turbine work is equal to the compressor work plus friction and accessory drive work. The turbine specific work can therefore be written

$$\frac{\Delta h_T'}{\theta_3} = \frac{\theta_1 \frac{\Delta h_C'}{\theta_1} + W}{\theta_3\left[1 + \left(\frac{f}{a}\right)_3\right]} \tag{42}$$

where W is the total of the specific work of the accessory drives and friction in Btu per pound of compressor-inlet air. Generally, W can be neglected.

Using the value of specific turbine work from equation (42), the fuel-air ratio $(f/a)_3$, and the equivalent turbine-inlet temperature θ_3, the temperature ratio across the turbine θ_4/θ_3 can be read from figure 7. For values of fuel-air ratio that are less than 0.01, the fuel-air correction lines can be extended for extrapolation. Normally, however, the range covered is adequate.

Turbojet-engine turbine pressure ratio. - The method used to determine the turbine pressure ratio depends on whether adiabatic or polytropic turbine efficiency is used, but figure 8 is used for the evaluation in either case. For the case where adiabatic efficiency is used, the work parameter $\Delta h_T'/\eta_T\theta_3$ is calculated from the equivalent specific work $\Delta h_T'/\theta_3$ and the adiabatic efficiency η_T. Using the proper values of the equivalent turbine-inlet temperature θ_3 and the fuel-air ratio $(f/a)_3$, the pressure ratio p_4'/p_3' is read directly from figure 8.

For the case where polytropic efficiency is used, the pressure ratio can be read directly from the curve, or interpolation for turbine polytropic efficiency can be eliminated by a simple calculation. In either case the quantity $(p_4'/p_3')^{\eta_T,\infty}$ is first read from figure 8 that corresponds to the equivalent turbine work $\Delta h_T'/\theta_3$, equivalent turbine-inlet temperature θ_3, and fuel-air ratio $(f/a)_3$ previously calculated. The pressure ratio p_4'/p_3' can then be either calculated or read from the curve corresponding to the proper polytropic efficiency.

It has been assumed in the discussion that the turbine work was a known quantity and that it was desired to calculate the pressure ratio. This will not always be the case. The curves can also be used for calculating turbine work or turbine efficiency from component tests.

Total fuel-air ratio for turbojet engine with afterburner. - From equation (14) it can be seen that

$$\left(\frac{f}{a}\right)_6 = \left(\frac{f}{a}\right)_5 + \left(\frac{f}{a}\right)^*\left[1 + 2.9\left(\frac{f}{a}\right)_5\right] \tag{43}$$

where the term $(f/a)^*$ is obtained from figure 6 for corresponding values of equivalent burner-inlet temperatures $\theta_5 = \theta_4$, burner-outlet temperature T_6', and burner efficiency $\eta_{B,5-6}$. For the case where there is no bleed air, $(f/a)_5 = (f/a)_3$. If the hydrogen-carbon ratio H/C is different from 0.167, the fuel-air ratio can be closely approximated, as explained previously, by dividing the value of $(f/a)^*$ read from the curve by the quantity 0.670 H/C + 0.888.

Turbojet-engine thrust with convergent-divergent exhaust nozzle. - The specific jet thrust is primarily a function of the pressure ratio across the nozzle, the gas temperature, and the nozzle efficiency. To a smaller degree the fuel-air ratio also affects the thrust. The pressure ratio across the nozzle p_6'/p_0 is calculated from

$$\frac{p_6'}{p_0} \equiv \frac{p_0'}{p_0}\frac{p_1'}{p_0'}\frac{p_2'}{p_1'}\frac{p_3'}{p_2'}\frac{p_4'}{p_3'}\frac{p_5'}{p_4'}\frac{p_6'}{p_5'} \tag{44}$$

where the pressure ratios p_3'/p_2', p_5'/p_4', and p_6'/p_5', for the primary burner, the diffuser downstream of the turbine, and the afterburner, respectively, are assigned values, usually based on experimental data.

The gross specific thrust corrected to jet nozzle conditions can be evaluated from figure 9 as a function of p_6'/p_0, θ_6, and $(f/a)_6$, where

$$\frac{F}{w_6\sqrt{\theta_6}} = C\sqrt{\eta_n}\,\frac{F^*}{w_6\sqrt{\theta_6\eta_n}} \tag{45}$$

For the case where there is no afterburner,

$$\theta_6 = \theta_4 \equiv \theta_3\frac{\theta_4}{\theta_3} \tag{46}$$

and

$$\left(\frac{f}{a}\right)_6 = \left(\frac{f}{a}\right)_3 \tag{47}$$

The net specific thrust corrected to compressor-inlet conditions is

$$\frac{F_N}{w_1\sqrt{\theta_1}} = \frac{1}{\sqrt{\theta_1}}\left\{\sqrt{\theta_6}\left[1 + \left(\frac{f}{a}\right)_6\right]\frac{F}{w_6\sqrt{\theta_6}} - 1.523\ M_0\sqrt{T_0}\right\} \tag{48}$$

Turbojet-engine thrust with convergent exhaust nozzle. - For values of $p_6'/p_0 < 2.0$, the jet thrust is obtained in exactly the same manner as for a convergent-divergent nozzle. For values of $p_6'/p_0 > 2.0$, the quantity $F^*/w_6\sqrt{\theta_6}$ is read from figure 10 as a function of p_6'/p_0 and η_n. The correction factor $\overline{C}$ is read as a function of θ_6 and $(f/a)_6$. The gross specific thrust corrected to jet nozzle conditions is

$$\frac{F}{w_6\sqrt{\theta_6}} = \overline{C}\,\frac{F^*}{w_6\sqrt{\theta_6}} \tag{49}$$

The specific thrust corrected to compressor-inlet conditions is calculated by equation (48).

Turbojet-engine specific fuel consumption. - The corrected thrust specific fuel consumption in pounds of fuel per hour per pound of thrust is

$$TSFC = \frac{3600\ w_f}{F_N\sqrt{\theta_1}} = \frac{3600\left(\frac{f}{a}\right)_6}{\theta_1\left(\frac{F_N}{w_1\sqrt{\theta_1}}\right)} \tag{50}$$

Turboprop-engine turbine work, pressure ratio, and temperature ratio. - The pressure level at the turbine exit p_4' is usually a set value that is determined by the amount of jet thrust desired or the ambient exhaust pressure. This pressure and the turbine-inlet temperature are then the primary factors determining the turbine work. The turbine pressure ratio is obtained from

$$\frac{p_4'}{p_3'} \equiv \frac{\dfrac{p_4'}{p_0}}{\dfrac{p_0'}{p_0}\dfrac{p_1'}{p_0'}\dfrac{p_2'}{p_1'}\dfrac{p_3'}{p_2'}} \tag{51}$$

The turbine work is then obtained through use of figure 8 for either adiabatic or polytropic efficiency. The temperature ratio across the turbine is obtained from figure 7 and the turbine work.

Turboprop-engine shaft power. - The specific shaft power is obtained from the difference between the turbine power and the compressor power with allowance given to gearbox efficiency:

$$\frac{HP}{w_1\theta_1} = \frac{J\eta_G}{550\ \theta_1}\left\{\left[1 + \left(\frac{f}{a}\right)_3\right]\theta_3\ \frac{\Delta h_T'}{\theta_3} - \theta_1\ \frac{\Delta h_C'}{\theta_1} - W\right\} \tag{52}$$

Turboprop-engine specific fuel consumption. - The corrected brake specific fuel consumption in pounds of fuel per horsepower-hour is

$$BSFC = \frac{3600\ w_f}{HP} = \frac{3600\left(\frac{f}{a}\right)_3}{\theta_1\ \frac{HP}{w_1\theta_1}} \tag{53}$$

Cycle Calculations with Compressor Bleed and Turbine Cooling

The use of the curves is the same whether air is bled from the compressor or not; consequently, their use will not be further discussed. The essential difference between the calculations with compressor bleed and those without is in accounting for variations in mass flow through the engine and temperature variations due to mixing air in with the hot gas or removing heat through the turbine blades.

Many of the effects due to mixing of cooling air with the exhaust gases and the heat that is removed because of cooling are of very small magnitude. Several methods are possible for handling the calculation procedure:

(1) It can be assumed that air used for cooling each stage is discharged into the exhaust gases at the exit of the stage and becomes part of the working gases for the following stages. For this case there is also a heat reduction due to cooling of the working gases through the stage. This heat is restored at the stage exit when the cooling air mixes in with the working gases. The gas temperature at the stage exit is reduced, however, by dilution from the cooling air. There is also a mixing pressure loss when the cooling air mixes with the gases.

(2) It can be assumed that the turbine is divided into a section of cooled stages and a section of uncooled stages and that all the air used for cooling is mixed with the working gases at the exit of the cooled stages, with the attendant mixing losses, dilution, and restoration of heat that was given up by the blades to the cooling air.

(3) Since the cooling air is discharged from the blades at a low energy level relative to the working gases, it is questionable that much

additional turbine work can be obtained from the cooling air in succeeding turbine stages. Any work that might be obtained could possibly overcome mixing pressure losses. Based on these conditions, it would appear feasible to assume that all cooling air mixes with the working gases at the turbine exit, so that no turbine work is obtained from the gases, but the air is available for jet thrust.

(4) It could be assumed that the accuracy of the calculations does not warrant the inclusion of effects of heat rejection from the blades to the cooling air or the effects of additional pumping power on the cooling air as the air passes through the turbine rotor. For this case the only effect of bleeding air for cooling purposes would be a decrease in mass flow of the working gases in the turbine relative to the mass flow in the compressor.

In the calculation methods presented herein it was felt that known effects on engine performance should be included where possible. For this reason the effect of turbine rotor cooling-air pumping power is included. In addition, provision is made to include the effects of heat rejection from the turbine blades to the cooling air. In many cases, particularly for the turbojet engine, however, this heat rejection has a negligible effect on engine performance; consequently, the user of the curves presented can omit all heat-rejection terms if he so desires. The methods presented neglect any positive work that might be obtained from the cooling air (assumption (3)), because it is questionable if work obtained would be greater than mixing and other losses that may be involved. Experimental data concerning this effect on turbine performance are presently lacking. If the user of the curves wishes to include the effect of work obtained from cooling air on turbine stages following the cooled stage, alteration of the equations given is a relatively simple matter. The total turbine power would be handled by individual stages rather than lumping all the stages together.

In the discussion of calculation methods that follows, only the portions of the procedure that are different from the case without the compressor bleed or turbine cooling are discussed. In addition, it should be stated that the use of the curves is not limited to the calculation methods presented herein. The curves are equally useful for other engine cycles which also involve burners, compressors, turbines, or exhaust nozzles. As an example, the curves could also be used for cycle analysis of ducted-fan engines.

Compressor work and temperature ratio. - The compressor work for the case with bleed is the sum of the work on the main body of air passing through the compressor $(\Delta h_c'/\theta_1)(w_1 - w_b)$ plus the work on the air that is bled off for cooling or other purposes $(\Delta h_b'/\theta_1)(w_b)$. The values of $\Delta h_c'/\theta_1$ and $\Delta h_b'/\theta_1$ are obtained from figure 4 and correspond to the

pressure ratios p_2'/p_1' and p_b'/p_1', respectively. If the bleed air is bled from the compressor discharge, then $p_b'/p_1' = p_2'/p_1'$, and the compressor work is calculated in the same manner as explained previously for Cycle Calculations without Compressor Bleed and Turbine Cooling.

Values of compressor temperature ratio θ_b/θ_1 and θ_2/θ_1 are read from figure 5 corresponding to the compressor equivalent work values $\Delta h_b'/\theta_1$ and $\Delta h_c'/\theta_1$, respectively.

Turbojet-engine turbine work, turbine temperature ratio, and turbine pressure ratio. - For the case where there are cooled stages in the turbine, the temperature of the gases will be reduced by the removal of heat due to cooling. The reduction of gas temperature due to heat removal can be closely approximated by

$$\Delta\theta \approx 0.00638 \frac{Q}{w_3} \tag{54}$$

Because of the small magnitude of this correction, a refinement for variations in specific heat due to temperature level and fuel-air ratio is not warranted. For most purposes, sufficient accuracy is obtained by assuming that the entire heat removal takes place at the turbine inlet; then

$$\theta_{3,r} = \theta_3 - \Delta\theta \tag{55}$$

The effect of heat removal on the efficiency of a simple gas-turbine cycle is discussed in references 7 to 9. Reference 7 considered removal of heat both at the inlet and exit of the turbine stage. Since the heat removal occurs in the boundary layer, it is doubtful whether the main working fluid is affected until after the blade row. Probably the most accurate solution, therefore, would be removal of half the heat before the stage due to stator cooling and removal of the other half of the heat after the stage due to rotor cooling. Calculations show that the final results are affected only slightly wherever the heat rejection is assumed to occur; and the calculations can be simplified, particularly for multistage turbines, by assuming that all heat rejection occurs at the turbine inlet.

Actually, the effect of heat removal on air-cooled turbojet engines is negligible, so that for most purposes calculations do not require the use of terms involving $\Delta\theta$. This conclusion is somewhat at variance with the results in references 7 to 9, because unpublished calculations conducted at the NACA show that the heat rejection due to turbine cooling is only from one-third to one-half that calculated by the method of reference 7. The terms required for consideration of heat removal are

included in the equations herein, and it will be left to the user of the curves to decide whether the heat-removal terms should be included in his calculations.

The equivalent turbine work is obtained from

$$\frac{\Delta h_T'}{\theta_{3,r}} = \frac{\theta_1\left(1 - \frac{w_b}{w_1}\right)\frac{\Delta h_C'}{\theta_1} + \theta_1 \frac{w_b}{w_1}\frac{\Delta h_b'}{\theta_1} + \frac{U_T^2}{gJ}\frac{w_{a,R}}{w_1} + W}{\theta_{3,r}\left[1 + \left(\frac{f}{a}\right)_3\right]\left(1 - \frac{w_b}{w_1}\right)} \tag{56}$$

where

$$w_b = w_{a,R} + w_{a,S} + w_{ov} \tag{57}$$

and $\frac{U_T^2}{gJ}\frac{w_{a,R}}{w_1}$ is the total cooling-air pumping work for all the cooled stages in the turbine rotor.

In equation (56) it is assumed that all bleed air is bled from the same point on the compressor. By the use of additional terms in the numerator, it is obvious that it would be possible to account for compressor bleed at various points in the compressor. As an example, assume that the overboard bleed air was bled from the compressor discharge while the rotor and stator cooling air were bled at the pressure ratio p_b'/p_1'. For this case, the equivalent turbine work would be

$$\frac{\Delta h_T'}{\theta_{3,r}} = \frac{\theta_1\left(1 - \frac{w_b}{w_1} + \frac{w_{ov}}{w_1}\right)\frac{\Delta h_C'}{\theta_1} + \theta_1\left(\frac{w_{a,R}}{w_1} + \frac{w_{a,S}}{w_1}\right)\frac{\Delta h_b'}{\theta_1} + \frac{U_T^2}{gJ}\frac{w_{a,R}}{w_1} + W}{\theta_{3,r}\left[1 + \left(\frac{f}{a}\right)_3\right]\left(1 - \frac{w_b}{w_1}\right)} \tag{56a}$$

The turbine temperature ratio $\theta_4/\theta_{3,r}$ and expansion ratio p_4'/p_3' are read from figures 7 and 8 corresponding to the value of $\Delta h_T'/\theta_{3,r}$ obtained from equation (56). For the case where cooling air from the cooled turbine is mixed with the working fluid gases downstream of the turbine, the temperature downstream of the cooled turbine is given by

$$\theta_{4,r} =$$

$$\frac{\left[1+\left(\frac{f}{a}\right)_3\right]\left(1-\frac{w_b}{w_1}\right)\theta_4+\left(\frac{w_{a,R}}{w_1}+\frac{w_{a,S}}{w_1}\right)\theta_b+\frac{w_{a,R}}{w_1}\frac{U_T^2}{518.7gJc_p}+\Delta\theta\left[1+\left(\frac{f}{a}\right)_3\right]\left(1-\frac{w_b}{w_1}\right)}{\left[1+\left(\frac{f}{a}\right)_3\right]\left(1-\frac{w_b}{w_1}\right)+\frac{w_{a,R}}{w_1}+\frac{w_{a,S}}{w_1}} \tag{58}$$

where

$$\theta_4 \equiv \theta_{3,r}\frac{\theta_4}{\theta_{3,r}} \tag{59}$$

A slight approximation is involved in equation (58) by assuming constant specific heat throughout the equation. This assumption has a negligible effect on the final results.

Total fuel-air ratio for turbojet with afterburner. - The total fuel-air ratio is calculated in the same manner as for Cycle Calculations without Compressor Bleed and Turbine Cooling using equation (43). For the case with compressor bleed, however, the fuel-air ratio at station 5 is different from that at station 3, as shown in the following equation:

$$\left(\frac{f}{a}\right)_5 = \frac{\left(\frac{f}{a}\right)_3\left(1-\frac{w_b}{w_1}\right)}{\left(1-\frac{w_b}{w_1}\right)+\frac{w_{a,R}}{w_1}+\frac{w_{a,S}}{w_1}} \tag{60}$$

and with a cooled turbine

$$\theta_5 = \theta_{4,r} \tag{61}$$

Turbojet-engine thrust. - The gross specific thrust corrected to exhaust-nozzle conditions is obtained in the same manner as for Cycle Calculations without Compressor Bleed and Turbine Cooling. The net specific thrust corrected to compressor-inlet conditions is given by

$$\frac{F_N}{w_1\sqrt{\theta_1}} = \frac{1}{\sqrt{\theta_1}}\left(\sqrt{\theta_6}\left\{\left[1+\left(\frac{f}{a}\right)_6\right]\left(1-\frac{w_b}{w_1}\right)+\frac{w_{a,R}}{w_1}+\frac{w_{a,S}}{w_1}\right\}\frac{F}{w_6\sqrt{\theta_6}} - 1.523M_0\sqrt{T_0}\right) \tag{62}$$

Turbojet-engine specific fuel consumption. - Applying a correction to equation (50) for the air bled from the compressor,

$$TSFC = \frac{3600\ w_f}{F_N \sqrt{\theta_1}} = \frac{3600\left(\frac{f}{a}\right)_6\left(1 - \frac{w_b}{w_1} + \frac{w_{a,R}}{w_1} + \frac{w_{a,S}}{w_1}\right)}{\theta_1\left(\frac{F_N}{w_1 \sqrt{\theta_1}}\right)} \tag{63}$$

For afterburning engines, $(f/a)_6$ is obtained from equations (43) and (60). For nonafterburning engines,

$$\left(\frac{f}{a}\right)_6 = \frac{\left(\frac{f}{a}\right)_3\left(1 - \frac{w_b}{w_1}\right)}{1 - \frac{w_b}{w_1} + \frac{w_{a,R}}{w_1} + \frac{w_{a,S}}{w_1}} \tag{64}$$

Turboprop-engine turbine work, turbine temperature ratio, and turbine pressure ratio. - The turbine work and temperature ratio are calculated by the same method as in the section Cycle Calculations without Compressor Bleed and Turbine Cooling, except that for a given turbine pressure ratio p'_4/p'_3 the resulting specific turbine work is $\Delta h'_T/\theta_{3,r}$, where $\theta_{3,r}$ is obtained from equation (55). It is more important to include the effects of heat removal from the gas due to cooling for a turboprop engine than it is for a turbojet engine.

Turboprop-engine shaft power. - The specific shaft power is calculated from

$$\frac{HP}{w_1\theta_1} =$$

$$\frac{J\eta_G}{550\theta_1}\left\{\left[1+\left(\frac{f}{a}\right)_3\right]\left(1-\frac{w_b}{w_1}\right)\theta_{3,r}\,\frac{\Delta h'_T}{\theta_{3,r}} - \left(1-\frac{w_b}{w_1}\right)\theta_1\,\frac{\Delta h'_C}{\theta_1} - \frac{w_b}{w_1}\,\theta_1\,\frac{\Delta h'_b}{\theta_1} - \frac{w_{a,R}}{w_1}\,\frac{U_T^2}{gJ} - W\right\} \tag{65}$$

Turboprop-engine specific fuel consumption. - Applying a correction to equation (53) for air bled from the compressor,

$$BSFC = \frac{3600\ w_f}{HP} = \frac{3600\left(\frac{f}{a}\right)_3\left(1 - \frac{w_b}{w_1}\right)}{\theta_1\left(\frac{HP}{w_1\theta_1}\right)} \tag{66}$$

ILLUSTRATIVE EXAMPLE

The details of a numerical example are presented herein to explain more clearly the use of the charts for evaluating the performance of a turbojet engine with various types of compressor bleed. The example chosen uses 3 percent of the compressor air for cooling the turbine stator blades and 3 percent for cooling the turbine rotor blades. This air is bled from the compressor at a pressure ratio of 3.0. Overboard air is bled from the compressor discharge and is assumed to be 1 percent of the compressor-inlet air.

In the determination of the turbine work, consideration is given to the amount of heat removed from the gas stream due to cooling and also to the work required to pump the cooling air from the rotor hub to the tip of the turbine rotor blades. The amount of heat removed from the gas stream per pound of gas Q/w_3 was computed and found to be 4.84 Btu per pound. Friction and accessory drive work were neglected. The flight conditions and engine specifications are summarized as follows:

Altitude, ft	--	50,000
Flight Mach number	M_0	2.0
Ram recovery	p_1'/p_0'	0.85
Cooling-air-bleed pressure ratio	p_b'/p_1'	3.0
Compressor pressure ratio	p_2'/p_1'	6.0
Primary-burner pressure ratio	p_3'/p_2'	0.95
Tail-cone diffuser pressure ratio	p_5'/p_4'	0.95
Afterburner pressure ratio	p_6'/p_5'	0.90
Heat removed from combustion gases by rotor and stator cooling, Btu/sec	Q/w_3	4.84
Ambient temperature, $^\circ R$	T_0	390
Turbine-inlet temperature, $^\circ R$	T_3'	2500
Afterburner temperature, $^\circ R$	T_6'	3500
Turbine tip speed, ft/sec	U_T	1200
Friction and accessory drive work	W	0
Turbine rotor cooling-air-flow ratio	$w_{a,R}/w_1$	0.03
Turbine stator cooling-air-flow ratio	$w_{a,S}/w_1$	0.03
Overboard-bleed ratio	w_{ov}/w_1	0.01
Primary-burner efficiency	$\eta_{B,2-3}$	0.98
Afterburner efficiency	$\eta_{B,5-6}$	0.90
Compressor adiabatic efficiency	η_C	0.88
Turbine polytropic efficiency	$\eta_{T,\infty}$	0.85
Convergent-divergent nozzle efficiency	η_n	0.95

The numerical example is presented in tabular form:

Quantity to be evaluated	Quantities, equations, and curves required	Numerical value of quantity being evaluated
θ_1	M_0, altitude, and fig. 2	1.354
p_0'/p_0	M_0, altitude, and fig. 3	7.86
$\eta_C \Delta h_C'/\theta_1$	θ_1, p_2'/p_1', and fig. 4	83.0 Btu/lb
$\Delta h_C'/\theta_1$	$\eta_C \Delta h_C'/\theta_1$, η_C, and eq. (39)	94.3 Btu/lb
$\eta_C \Delta h_b'/\theta_1$	θ_1, p_b'/p_1', and fig. 4	45.5 Btu/lb
$\Delta h_b'/\theta_1$	$\eta_C \Delta h_b'/\theta_1$, η_C, and eq. (39)	51.7 Btu/lb
θ_2/θ_1	θ_1, $\Delta h_C'/\theta_1$, and fig. 5	1.738
θ_2	θ_1, θ_2/θ_1, and eq. (40)	2.353
θ_b/θ_1	θ_1, $\Delta h_b'/\theta_1$, and fig. 5	1.408
θ_b	θ_1, θ_b/θ_1, and $\theta_b \equiv \theta_1(\theta_b/\theta_1)$	1.906
$\eta_{B,2\text{-}3}(f/a)_3$	θ_2, T_3', and fig. 6	0.02030
$(f/a)_3$	$\eta_{B,2\text{-}3}$, $\eta_{B,2\text{-}3}(f/a)_3$, and eq. (41)	0.02071
$\Delta\theta$	Q/w_3 and eq. (54)	0.03
θ_3	T_3' and $\theta_3 \equiv T_3'/518.7$	4.82
$\theta_{3,r}$	θ_3, $\Delta\theta$, and eq. (55)	4.79
w_b/w_1	$w_{a,R}/w_1$, $w_{a,S}/w_1$, w_{ov}/w_1, and eq. (57)	0.07
$\Delta h_T'/\theta_{3,r}$	θ_1, w_b/w_1, $w_{a,R}/w_1$, $w_{a,S}/w_1$, w_{ov}/w_1, $\Delta h_C'/\theta_1$, $\Delta h_b'/\theta_1$, U_T, $\theta_{3,r}$, $(f/a)_3$, and eq. (56a)	27.70 Btu/lb
$\theta_4/\theta_{3,r}$	$\theta_{3,r}$, $(f/a)_3$, $\Delta h_T'/\theta_{3,r}$, and fig. 7	0.817
θ_4	$\theta_4/\theta_{3,r}$, $\theta_{3,r}$, and eq. (59)	3.91
$\theta_{4,r}$	θ_4, θ_b, $\Delta\theta$, w_b/w_1, $w_{a,R}/w_1$, $w_{a,S}/w_1$, U_T, $(f/a)_3$, $c_p = 0.25$, and eq. (58)	3.83
θ_5	$\theta_5 = \theta_{4,r}$	3.83
p_4'/p_3'	$\Delta h_T'/\theta_{3,r}$, $\theta_{3,r}$, $\eta_{T,\infty}$, $(f/a)_3$, and fig. 8	0.364
$(f/a)_5$	$(f/a)_3$, w_b/w_1, $w_{a,R}/w_1$, $w_{a,S}/w_1$, and eq. (60)	0.01946
$\eta_{B,5\text{-}6}(f/a)^*$	θ_5, T_6', $\eta_{B,5\text{-}6}$, and fig. 6	0.02736
$(f/a)^*$	$\eta_{B,5\text{-}6}$, $\eta_{B,5\text{-}6}(f/a)^*$, and $(f/a)^* \equiv \eta_{B,5\text{-}6}(f/a)^*/\eta_{B,5\text{-}6}$	0.03040

Quantity to be evaluated	Quantities, equations, and curves required	Numerical value of quantity being evaluated
$(f/a)_6$	$(f/a)_5$, $(f/a)^*$, and eq. (43)	0.05156
p_6'/p_0	p_0'/p_0, p_1'/p_0', p_2'/p_1', p_3'/p_2', p_4'/p_3', p_5'/p_4', p_6'/p_5', and eq. (44)	11.85
θ_6	T_6' and $\theta_6 \equiv T_6'/518.7$	6.748
$F^*/w_6\sqrt{\theta_6\eta_n}$	p_6'/p_0, θ_6, and fig. 9	56.98 (lb)(sec)/lb
C	p_6'/p_0, $(f/a)_6$, and fig. 9	1.009
$F/w_6\sqrt{\theta_6}$	$F^*/w_6\sqrt{\theta_6\eta_n}$, C, η_n, and eq. (45)	56.04 (lb)(sec)/lb
$F_N/w_1\sqrt{\theta_1}$	θ_1, θ_6, T_0, M_0, $(f/a)_6$, $F/w_6\sqrt{\theta_6}$, w_b/w_1, $w_{a,R}/w_1$, $w_{a,S}/w_1$, and eq. (62)	78.2 (lb)(sec)/lb
TSFC	$(f/a)_6$, θ_1, w_b/w_1, $w_{a,R}/w_1$, $w_{a,S}/w_1$, $F_N/w_1\sqrt{\theta_1}$, and eq. (63)	1.736 lb/(hr)(lb)

CONCLUDING REMARKS

Curves were developed and analytical procedures were devised for a rapid graphical evaluation of engine or component performance for both turbojet and turboprop engines. The calculation procedure permits evaluation of the effects of compressor bleed for turbine cooling or other purposes. The use of the curves is not limited to the calculation methods presented. The curves are equally useful for other engine cycles involving burners, compressors, turbines, or exhaust nozzles. As an example, the curves could also be used for cycle analysis of ducted-fan engines.

The curves were calculated for a fuel hydrogen-carbon ratio of 0.167, which is generally applicable to jet-engine fuels, and effects of variations in specific heat are included. Except for extreme cases, the curves are accurate at this hydrogen-carbon ratio to at least 3° R in temperature and 1 percent in pressure ratio, fuel-air ratio, and specific thrust. For hydrogen-carbon ratios considerably different from 0.167 (in the range from 0.1 to 0.2), somewhat larger errors are possible. The curves are adequate, however, for nearly all cycle or component analyses and reduction of experimental data for gas temperatures up to 3000° R. Since the effects of dissociation were neglected, the curves should be used with caution at gas temperatures in excess of 3000° R.

Lewis Flight Propulsion Laboratory
National Advisory Committee for Aeronautics
Cleveland, Ohio, October 21, 1954

APPENDIX A

SYMBOLS

The following symbols are used in this report:

A	area, sq ft
BSFC	brake specific fuel consumption, lb/hp-hr
C	thrust-correction factor for convergent-divergent nozzle
$\overline{C}$	thrust-correction factor for convergent nozzle
c_p	specific heat at constant pressure, Btu/(lb)($^\circ$R)
F	gross thrust, lb
F_N	net thrust, lb
F^*	uncorrected thrust, F/C or F/$\overline{C}$, lb
f/a	fuel-air ratio
$(f/a)^*$	$\frac{(f/a)_6 - (f/a)_5}{1 + 2.9(f/a)_5}$
g	acceleration due to gravity, 32.174 ft/sec^2
$\overline{H}$	lower heating value of fuel, Btu/lb
H/C	fuel hydrogen-carbon ratio
HP	horsepower
h	enthalpy, Btu/lb, defined by $\int_{400^\circ R}^{T} c_p \, dT$
J	mechanical equivalent of heat, 778.2 ft-lb/Btu
M	Mach number
p	pressure, lb/sq ft
Q/w	heat rejection, Btu/lb

R	gas constant, ft-lb/(lb)($^{\circ}$R)
T	temperature, $^{\circ}$R
TSFC	thrust specific fuel consumption, lb/(hr)(lb)
U	tip speed, ft/sec
V	velocity, ft/sec
v	specific volume, cu ft/lb
W	specific work of accessory drives and friction, Btu/lb
w	flow rate, lb/sec
X	$h'_{A,\beta} - h'_{A,\alpha}$, Btu/lb
Y	$\frac{h'_{A,\beta} - h'_{A,\alpha} + \psi'_{h,\beta} - \psi'_{h,\alpha}}{h'_{A,\beta} - h'_{A,\alpha}}$
Z	$\overline{H} - \frac{h'_{A,\beta} + \psi'_{h,\beta} - h_f}{\eta_B}$, Btu/lb
γ	ratio of specific heats
η	component efficiency
θ	ratio of total temperature to NACA standard sea-level temperature, $T'/518.7^{\circ}$ R
ρ	density, lb/cu ft
φ	$\int_{400^{\circ}\,R}^{T} \frac{c_p}{T}\,dT$, Btu/(lb)($^{\circ}$R)
ψ_h	$\frac{(h - h_A)\left(1 + \frac{f}{a}\right)}{f/a}$, Btu/lb

Subscripts:

A	dry air, zero fuel-air ratio
a	cooling air

B	burner
b	total air bleed, or bleed point on compressor (see fig. 1)
C	compressor
f	fuel
G	gearbox
i	isentropic or ideal
n	exhaust nozzle
ov	overboard bleed
R	turbine rotor
r	after heat removal or replacement
S	turbine stator
T	turbine
α,β	any arbitrary stations
∞	small stage or polytropic
0,1,2,3, 4,5,6,7	stations in engine (see fig. 1)

Superscript:

	stagnation conditions

APPENDIX B

DERIVATION OF EQUATIONS USED IN PREPARATION OF CHARTS

Isentropic Compression or Expansion

For an isentropic process, the general energy equation is

$$J\,dh = v\,dp \tag{B1}$$

where

$$dh = c_p\,dT \tag{B2}$$

For a perfect gas,

$$pv = RT \tag{B3}$$

By combining equations (B1) to (B3) and integrating between the inlet station α and the exit station β,

$$\int_{T_\alpha}^{T_\beta} \frac{c_p}{T}\,dT = \frac{R}{J}\ln\left(\frac{p_\beta}{p_\alpha}\right) \tag{B4}$$

By defining

$$\varphi \equiv \int_{400^\circ\,R}^{T} \frac{c_p}{T}\,dT \tag{B5}$$

equation (B4) becomes

$$(\varphi_\beta - \varphi_\alpha)_i = \frac{R}{J}\ln\left(\frac{p_\beta}{p_\alpha}\right) \tag{B6}$$

which can also be written

$$\frac{p_\beta}{p_\alpha} = e^{\frac{J}{R}(\varphi_\beta - \varphi_\alpha)_i} \tag{B7}$$

Compression with Constant Polytropic Efficiency

The polytropic, or small stage, efficiency for a compression process is defined

$$\eta_{C,\infty} \equiv \frac{dh_i}{dh} \tag{B8}$$

$$\equiv \frac{v\ dp}{Jc_p\ dT} \tag{B9}$$

Combining equations (B3), (B5), and (B9) and integrating between stations α and β result in

$$\varphi_\beta - \varphi_\alpha = \frac{R}{J} \ln\left(\frac{p_\beta}{p_\alpha}\right)^{\frac{1}{\eta_{C,\infty}}} \tag{B10}$$

which can also be written

$$\left(\frac{p_\beta}{p_\alpha}\right)^{\frac{1}{\eta_{C,\infty}}} = e^{\frac{J}{R}(\varphi_\beta - \varphi_\alpha)} \tag{B11}$$

Expansion with Constant Polytropic Efficiency

The polytropic, or small stage, efficiency for an expansion process is defined

$$\eta_{T,\infty} \equiv \frac{dh}{dh_i} \tag{B12}$$

$$\equiv \frac{Jc_p\ dT}{v\ dp} \tag{B13}$$

Combining equations (B3), (B5), and (B13) and integrating between stations α and β result in

$$\varphi_\beta - \varphi_\alpha = \frac{R}{J} \ln\left(\frac{p_\beta}{p_\alpha}\right)^{\eta_{T,\infty}} \tag{B14}$$

which can also be written

$$\left(\frac{p_\beta}{p_\alpha}\right)^{\eta_{T,\infty}} = e^{\frac{J}{R}(\varphi_\beta - \varphi_\alpha)} \tag{B15}$$

Fuel-Air Ratio

The quantity of fuel required for a combustion process between stations α and β can be calculated from the following heat balance, which includes the weight of fuel $w_{f,\alpha}$ that has been burned in a previous combustion process:

$$(w_{f,\beta} - w_{f,\alpha})(\eta_B \overline{H} + h_f) = (w_A + w_{f,\beta})h'_\beta - (w_A + w_{f,\alpha})h'_\alpha \tag{B16}$$

Letting

$$\frac{f}{a} = \frac{w_f}{w_A}$$

$$\psi'_{h,\beta} = \frac{(h'_\beta - h'_{A,\beta})\left[1 + \left(\frac{f}{a}\right)_\beta\right]}{\left(\frac{f}{a}\right)_\beta}$$

$$\psi'_{h,\alpha} = \frac{(h'_\alpha - h'_{A,\alpha})\left[1 + \left(\frac{f}{a}\right)_\alpha\right]}{\left(\frac{f}{a}\right)_\alpha}$$

equation (B16) can be reduced to the form

$$\left(\frac{f}{a}\right)_\beta = \left(\frac{f}{a}\right)_\alpha + \frac{(h'_{A,\beta} - h'_{A,\alpha})\left[1 + \left(\frac{f}{a}\right)_\alpha \frac{h'_{A,\beta} - h'_{A,\alpha} + \psi'_{h,\beta} - \psi'_{h,\alpha}}{h'_{A,\beta} - h'_{A,\alpha}}\right]}{\eta_B \overline{H} - h'_{A,\beta} - \psi'_{h,\beta} + h_f} \tag{B17}$$

By defining groups of terms as follows:

$$X = h'_{A,\beta} - h'_{A,\alpha}$$

$$Y = \frac{h'_{A,\beta} - h'_{A,\alpha} + \psi'_{h,\beta} - \psi'_{h,\alpha}}{h'_{A,\beta} - h'_{A,\alpha}}$$

$$Z = \overline{H} - \frac{h'_{A,\beta} + \psi'_{h,\beta} - h_f}{\eta_B}$$

equation (B17) becomes

$$\left(\frac{f}{a}\right)_\beta = \left(\frac{f}{a}\right)_\alpha + \frac{X\left[1 + \left(\frac{f}{a}\right)_\alpha Y\right]}{\eta_B Z} \tag{B18}$$

REFERENCES

1. Bolz, Ray E.: Graphical Solution for Performance of Continuous Flow Jet Engines. Trans. SAE, vol. 1, no. 2, Apr. 1947, pp. 235-251.

2. Pinkel, Benjamin, and Karp, Irving M.: A Thermodynamic Study of the Turbojet Engine. NACA Rep. 891, 1947. (Supersedes NACA WR E-241.)

3. Pinkel, Benjamin, and Karp, Irving M.: A Thermodynamic Study of the Turbine-Propeller Engine. NACA Rep. 1114, 1953. (Supersedes NACA TN 2653.)

4. English, Robert E., and Wachtl, William W.: Charts of Thermodynamic Properties of Air and Combustion Products from 300° to 3500° R. NACA TN 2071, 1950.

5. Keenan, Joseph H., and Kaye, Joseph: Gas Tables - Thermodynamic Properties of Air, Products of Combustion and Component Gases, Compressible Flow Functions. John Wiley & Sons, Inc., 1948.

6. Zucrow, M. J.: Principles of Jet Propulsion and Gas Turbines. John Wiley & Sons, Inc., 1948.

7. Hawthorne, W. R., and Walker, Antonia B.: The Effect of Blade Cooling on Stage Efficiency of a Gas Turbine. Rep. No. 6574-2, Gas Turbine Lab., M.I.T., Mar. 15, 1949. (ONR Contract N5ori-78, Task Order 21, NR-220-010, Proj. DIC 6574.)

8. Hawthorne, W. R., and Walker, Antonia B.: The Effect of Blade Cooling on the Efficiency of a Multistage Turbine. Rep. No. 6574-3, Gas Turbine Lab., M.I.T., May 1949. (ONR Contract N5ori-78, Task Order 21, NR 220-010.)

9. Rohsenow, W. M.: The Effect of Turbine Blade Cooling on the Efficiency of a Simple Gas Turbine Power Plant. Tech. Rep. No. 4, Gas Turbine Lab., M.I.T., Jan. 1953. (ONR Contract N5ori-7862, NR-091-158, Proj. 6888.)

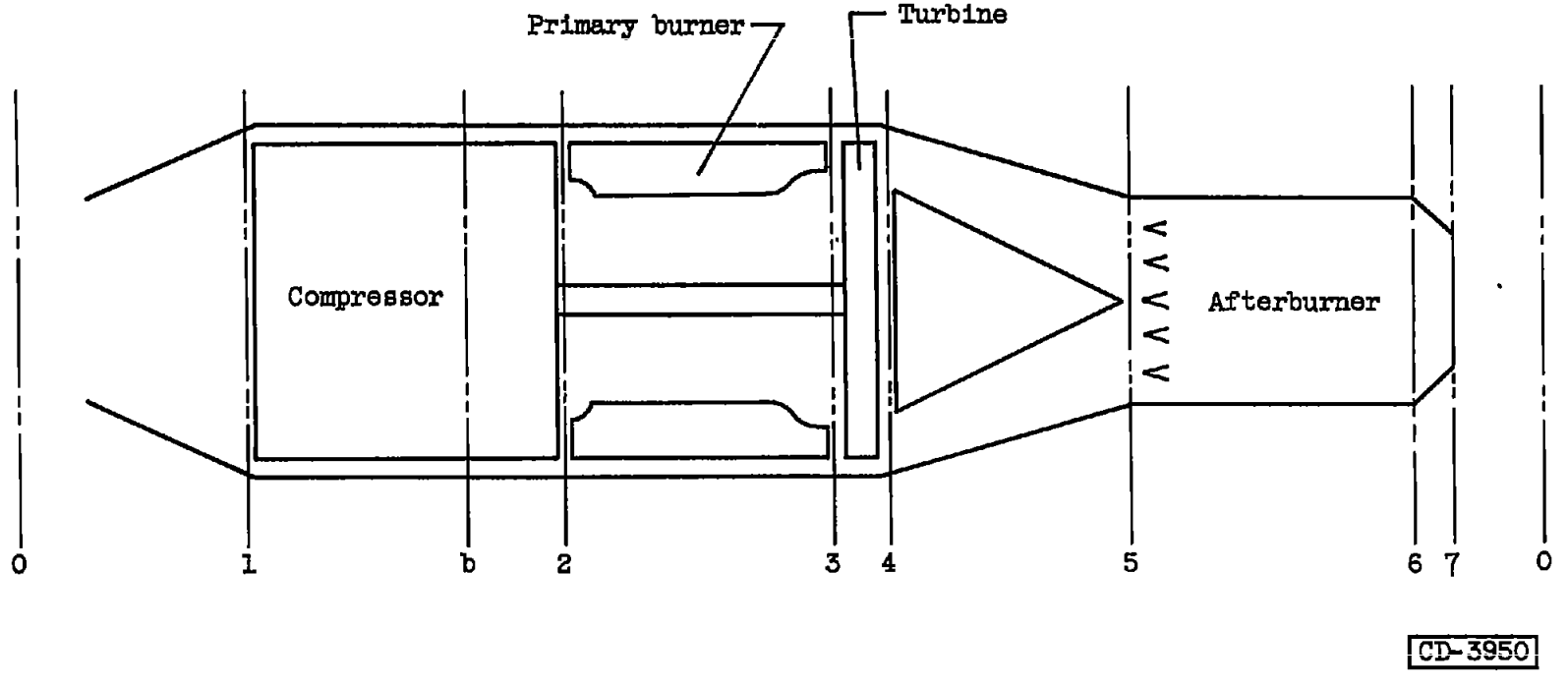

Figure 1. - Schematic sketch of engine showing calculation stations.

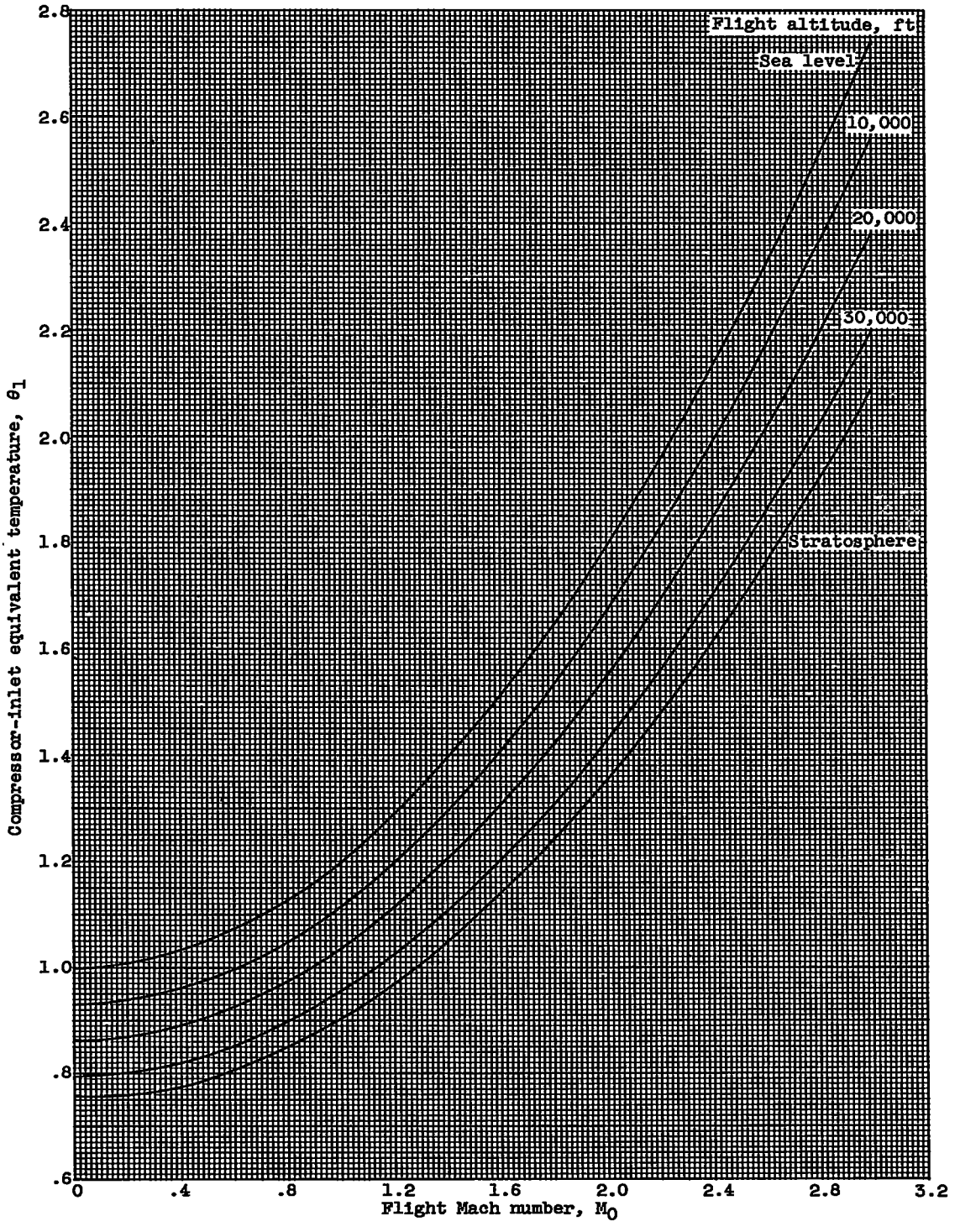

Figure 2. - Compressor-inlet equivalent temperature due to ram.

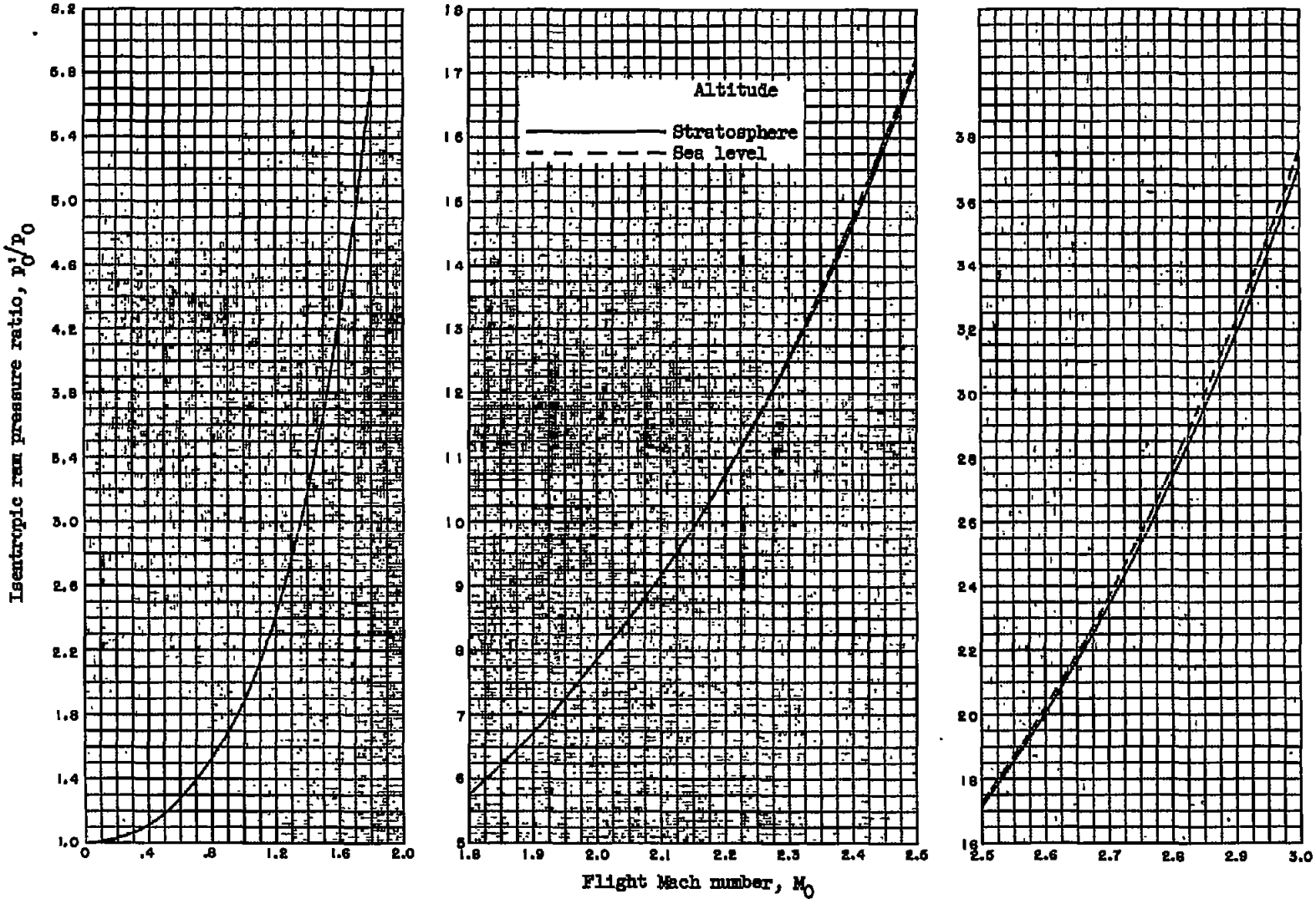

Figure 3. - Isentropic ram pressure ratio. (A large working copy of this chart may be obtained by using the request card bound in the back of the report.)

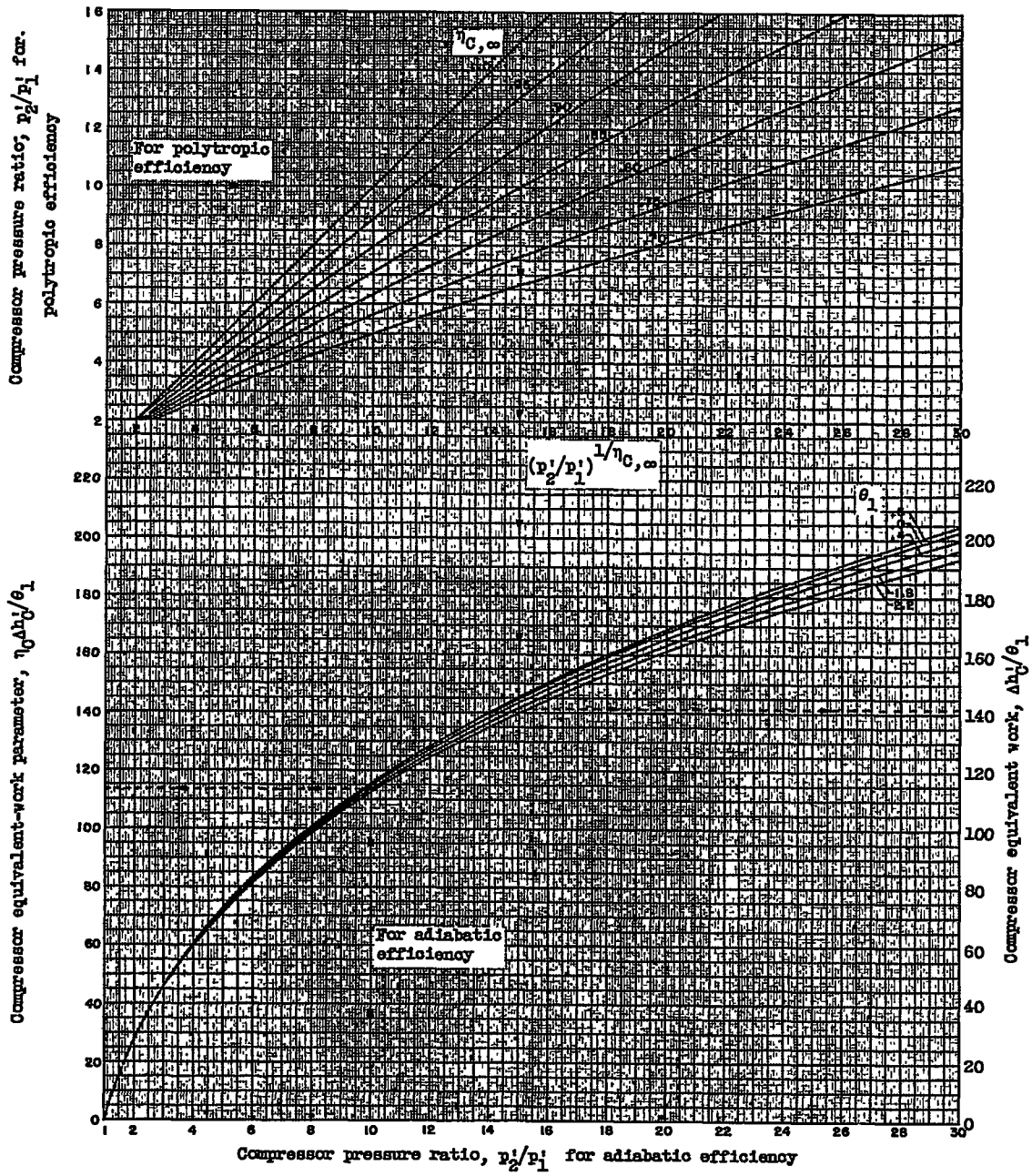

Figure 4. - Compressor work and pressure ratio. (A large working copy of this chart may be obtained by using the request card bound in the back of the report.)

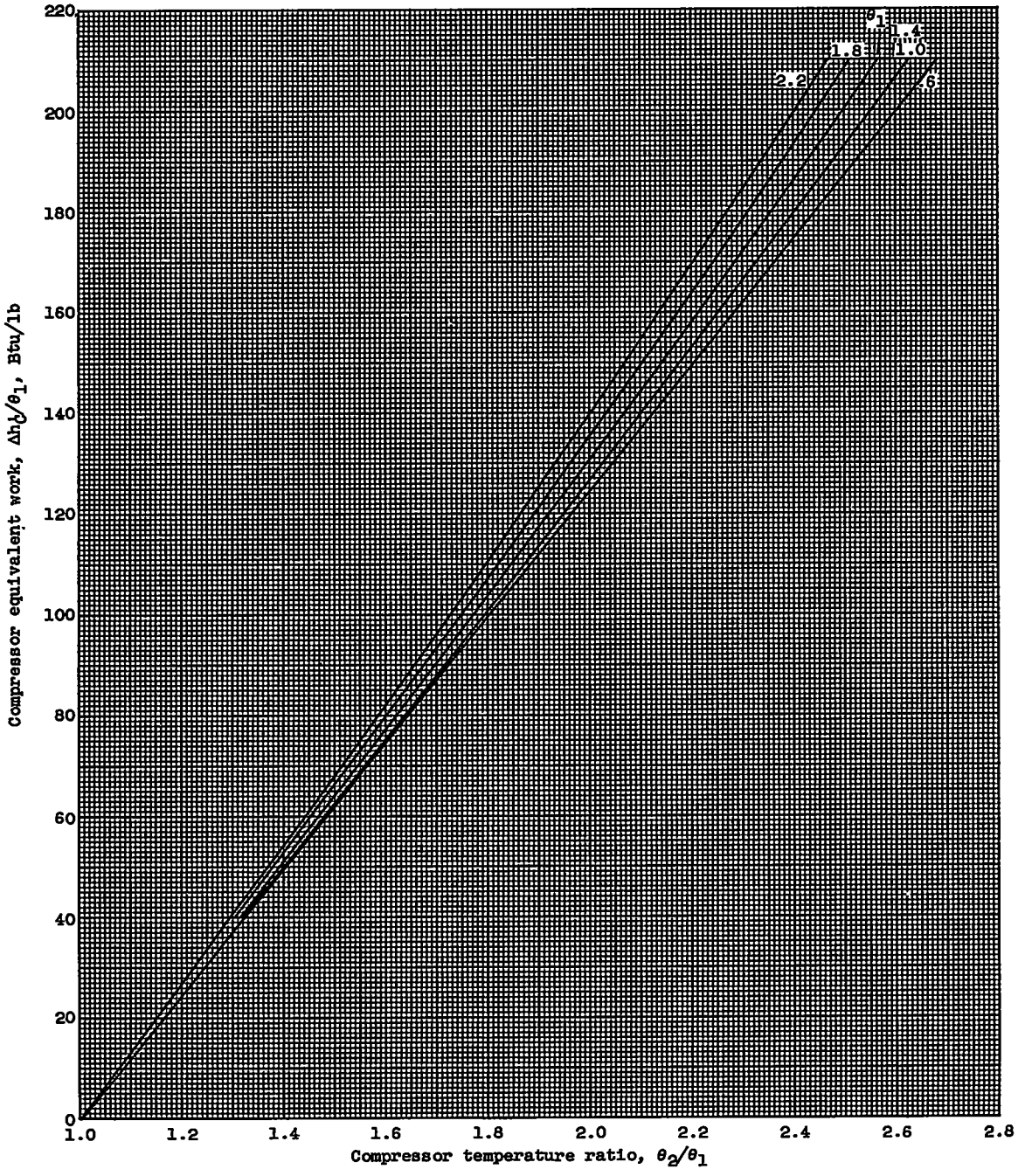

Figure 5. - Compressor work and temperature ratio.

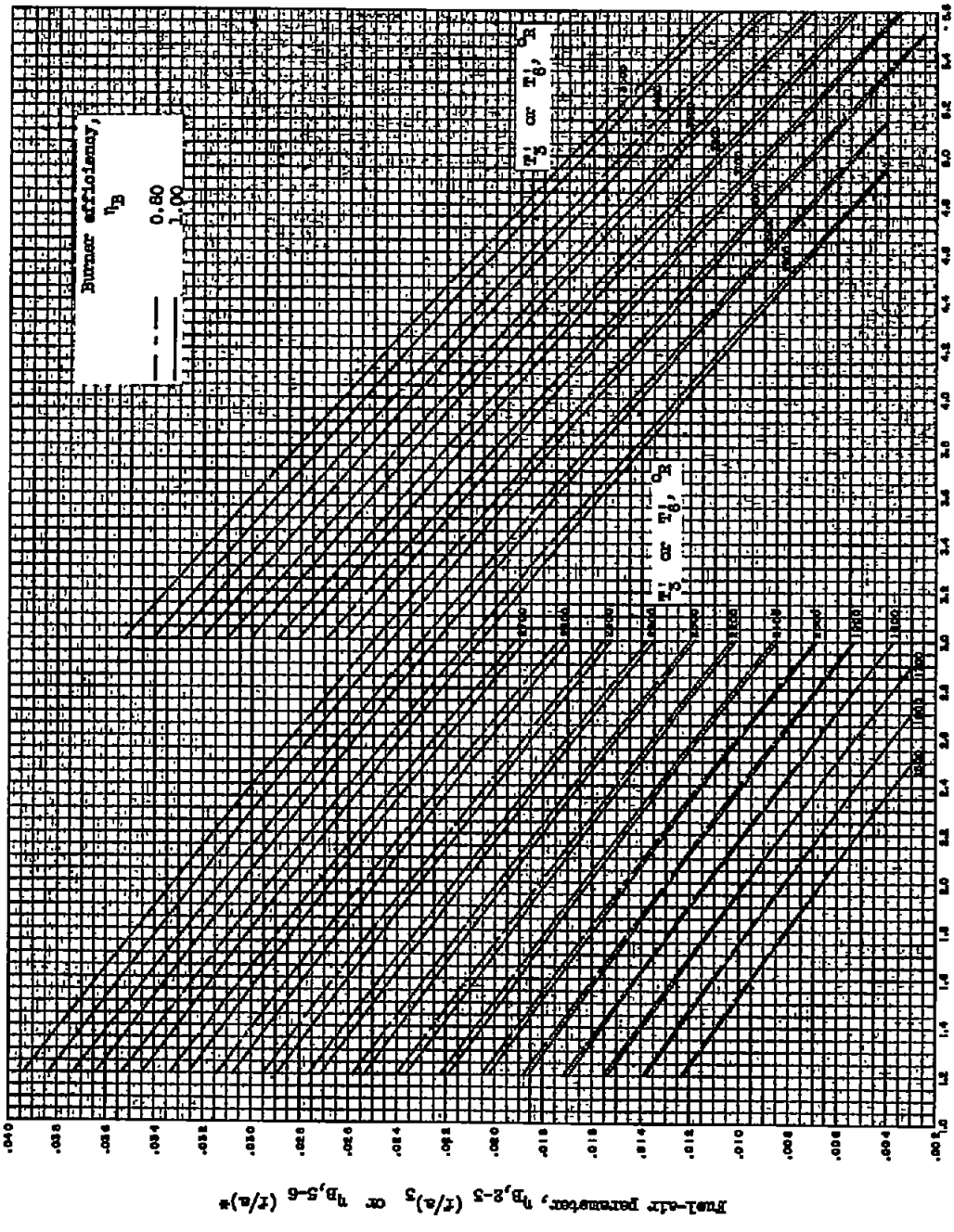

Figure 6. - Primary-burner and afterburner fuel-air ratio. (A large working copy of this chart may be obtained by using the request card bound in the back of the report.)

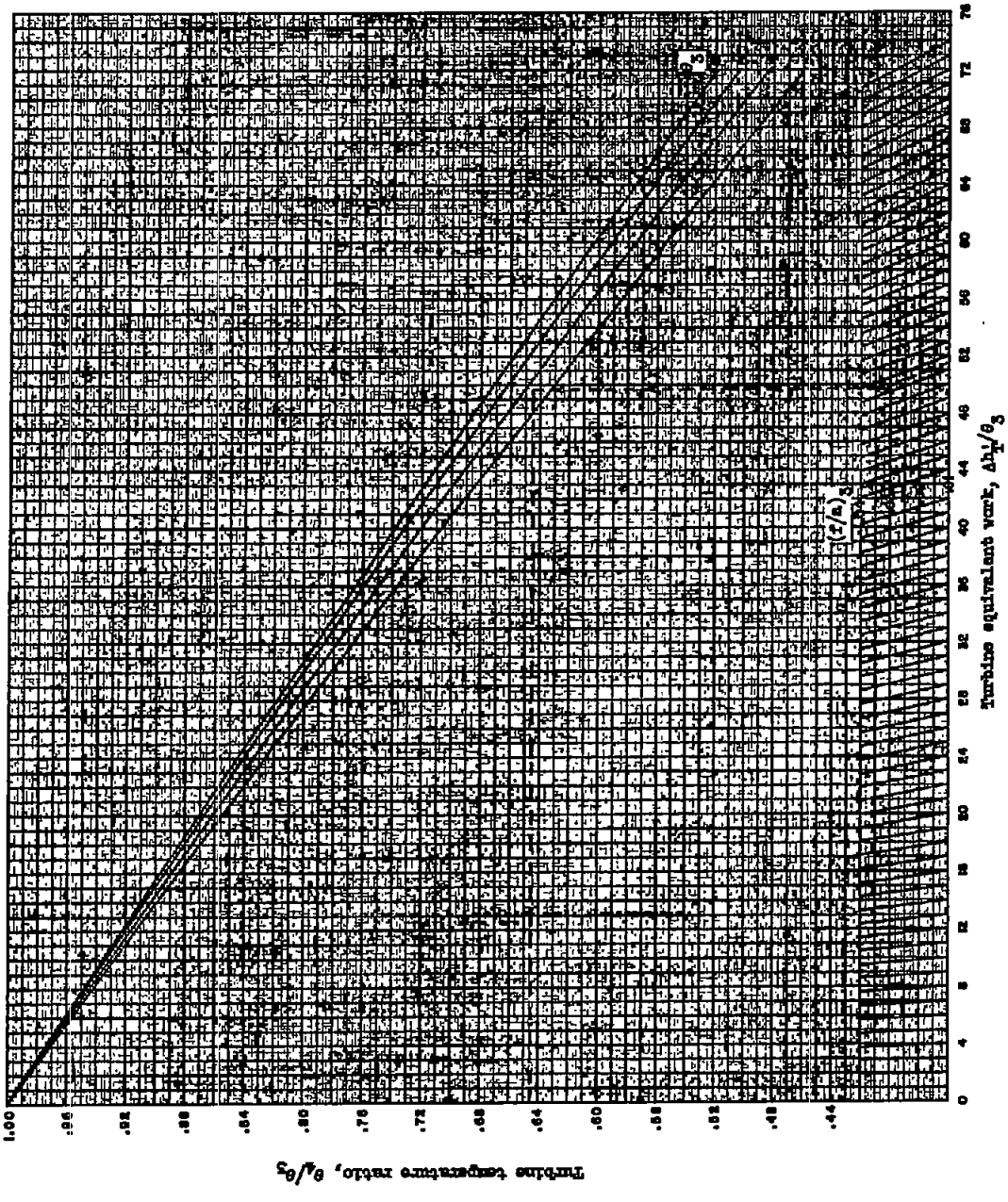

Figure 7. - Turbine work and temperature ratio. (A large working copy of this chart may be obtained by using the request card bound in the back of the report.)

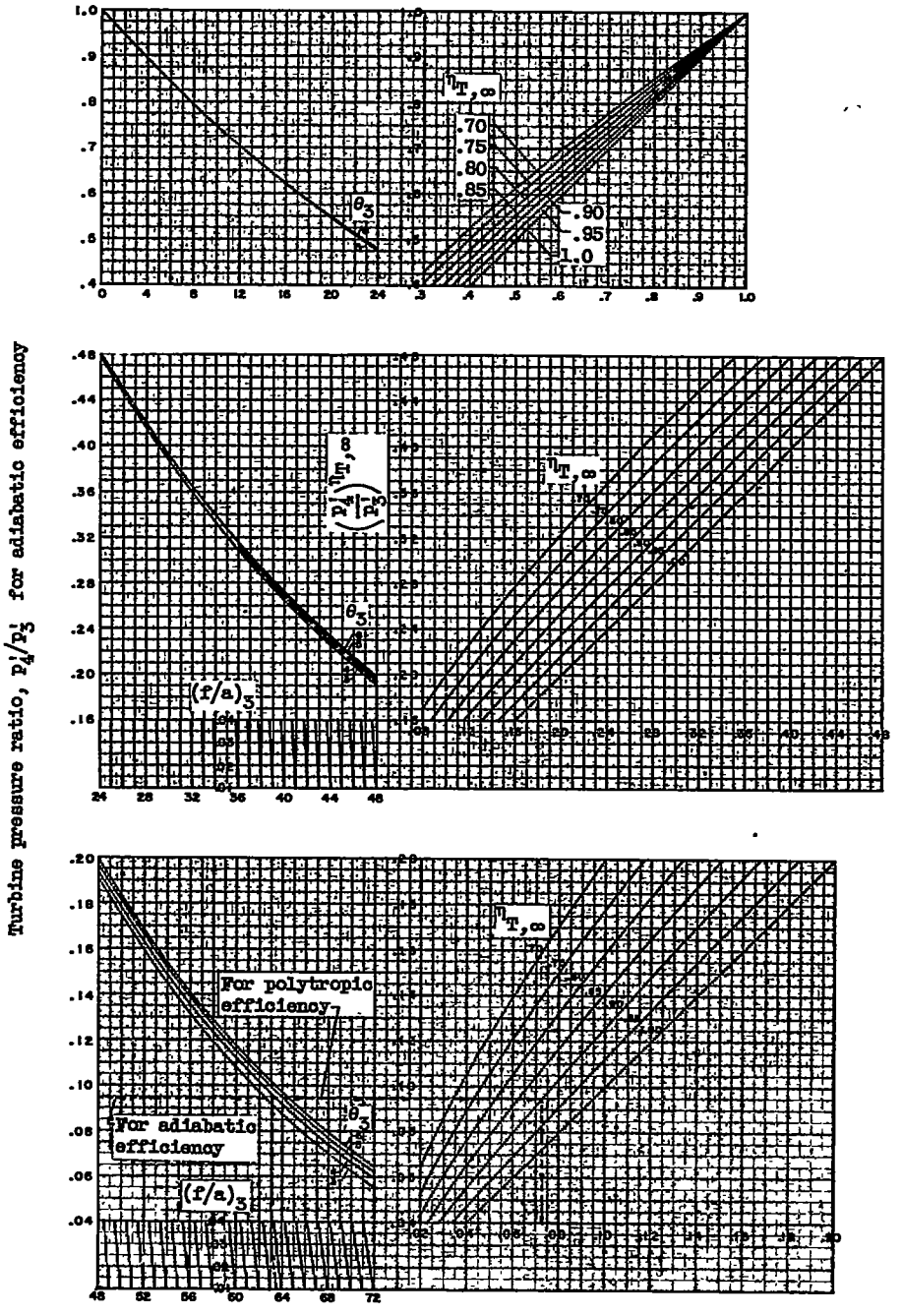

Figure 8. - Turbine work and pressure ratio. (A large working copy of this chart may be obtained by using the request card bound in the back of the report.)

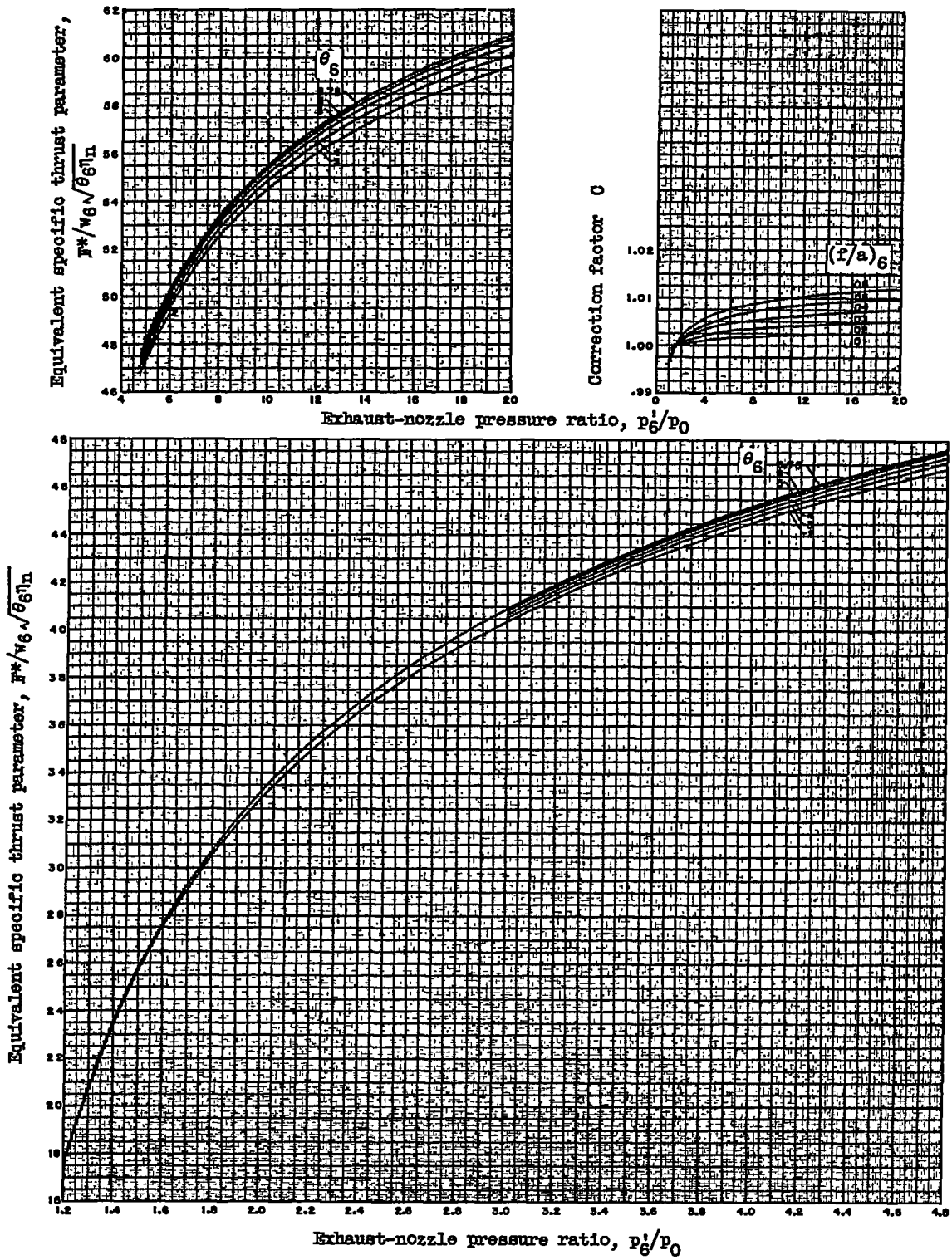

Figure 9. - Specific thrust for convergent-divergent exhaust nozzle. (A large working copy of this chart may be obtained by using the request card bound in the back of the report.)

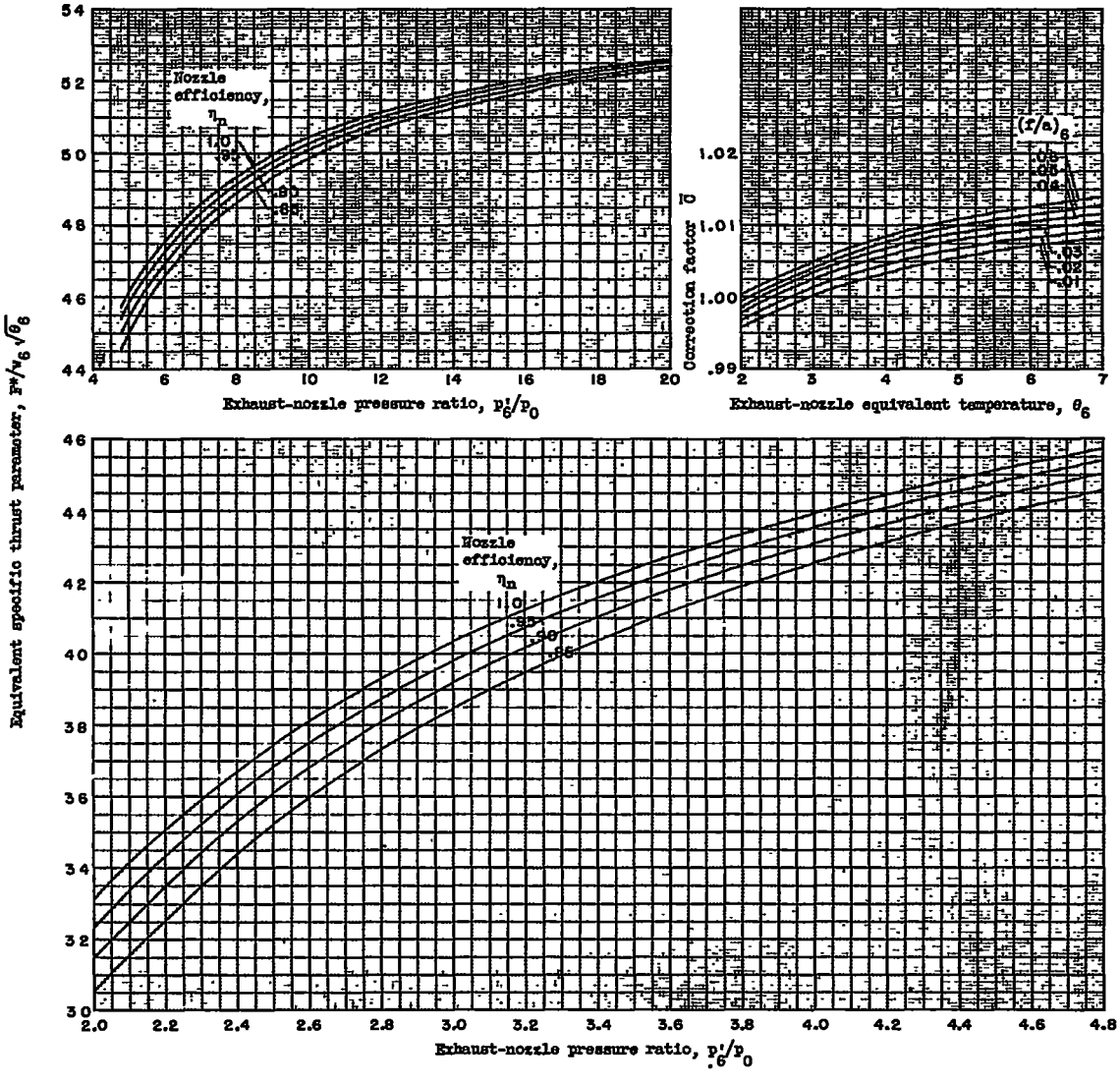

Figure 10. - Specific thrust for convergent exhaust nozzle. For pressure ratios less than 2, use figure 9 for convergent-divergent exhaust nozzle. (A large working copy of this chart may be obtained by using the request card bound in the back of the report.)